Supporting Information for

Thermally Labile Monoalkyl Phosphates and their Alkali Metal Derivatives: Synthesis and Solid State Supramolecular Aggregation

Anuj Kumar and Ramaswamy Murugavel*

Department of Chemistry, Indian Institute of Technology-Bombay, Powai, Mumbai-400076, India.
Fax: +91 22 2576 7152; Tel: +91 22 2576 7163; E-mail: rmv@chem.iitb.ac.in

Table S1. Surface property information in Hirshfeld for compound **2**.

Table S2. Surface property information in Hirshfeld for compound **4**.

Table S3. Fingerprint percentage of the total surface area for closed contact between atoms inside and outside the surface for compound **2**.

Table S4. Fingerprint percentage of the total surface area for closed contact between atoms inside and outside the surface for compound **4**.

Figure S25. FT-IR spectra of compounds **5–7** as KBr diluted discs.

Figure S26. ^{1}H NMR spectra of compounds $[(CF_3CH_2PO_4HLi)_3]_n$ (**5**), (Left) and $[(CF_3CH_2PO_4HNa)_2]_n$ (**6**) (Right) in D_2O.

Figure S27. ^{1}H NMR spectrum of compound $[CF_3CH_2OPO_3(Na_{0.5})_2)(CyNH_3)\cdot(H_2O)_6]_n$ (**7**) in D_2O.

Figure S28. ^{13}C NMR spectrum of compound $[(CF_3CH_2PO_4HLi)_3]_n$ (**5**) in D_2O.

Figure S29. ^{13}C NMR spectrum of compound $[(CF_3CH_2PO_4HNa)_2]_n$ (**6**) in D_2O.

Figure S30. ^{13}C NMR spectrum of compound $[CF_3CH_2OPO_3(Na_{0.5})_2)(CyNH_3)\cdot(H_2O)_6]_n$ (**7**) in D_2O.

Figure S31. ^{31}P NMR spectra of compounds **5–7** in (CD_3OD).

Figure S32. ^{19}F NMR spectrum of compound **5** (470 MHz) in (CD_3OD).

Figure S33. ^{19}F NMR spectrum of compound **6** (376 MHz) in (CD_3OD).

Figure S34. ^{19}F NMR spectrum of compound **7** (470 MHz), in (CD_3OD).

Figure S35. ^{7}Li NMR spectra of compounds $[(CF_3CH_2PO_4HLi)_3]_n$ (**5**) in (CD_3OD) (Left) and CP-MAS ^{7}Li NMR spectra (Right).

Figure S36. The CP-MAS ^{31}P NMR spectra of compounds **5**–**7**.

Figure S37. The CP-MAS ^{13}C NMR spectra of compounds $[(CF_3CH_2PO_4HLi)_3]_n$ (**5**); (left), and $[(CF_3CH_2PO_4HNa)_2]_n$ (**6**); (right).

Figure S52. DR-UV spectrum of the decomposed product of **6** at 650 °C.

Figure S53. SEM of the decomposed product of **5** at 650 °C.

Figure S54. SEM of the decomposed product of **6** at 650 °C.

Figure S55. (a) PXRD pattern of the as-synthesized organophosphates $[(CF_3CH_2PO_4HNa)_2]_n$ **(6)** mixed with $Co(OH)_2$ and ground at different time intervals; (b) PXRD patterns of the heterometal decomposition products obtained after pyrolysis at 800 °C, along with associated reference patterns of BT- $NaCoPO_4$ (ICDD, PDF number 01-087-1016).

Figure 56. FT-IR spectra of compound **5** mixed with $Co(OH)_2$, ground for 10 Minutes, 1h, and BT-800 °C ($LiCoPO_4$) as KBr diluted discs.

Figure S57. FT-IR spectra of compound **6** mixed with $Co(OH)_2$, ground for 10 Minutes, 1h, and BT-800 °C ($NaCoPO_4$) as KBr diluted discs.

Figure S58. DR UV-Vis absorption spectrum of $LiCoPO_4$.

Figure S59. DR UV-Vis absorption spectrum of $NaCoPO_4$.

Figure S60. SEM of the product of BT-$LiCoPO_4$ at 800 °C.

Figure S61. SEM of the product of BT-$NaCoPO_4$ at 800 °C.

Figure S62. Elemental analysis of $[(CF_3CH_2PO_4HLi)_3]_n$ **(5)**.

Figure S63. Elemental analysis of $[(CF_3CH_2PO_4HNa)_2]_n$ **(6)**.

Figure S64. Elemental analysis of $[CF_3CH_2OPO_3(Na_{0.5})_2(CyNH_3)\cdot(H_2O)_6]_n$ (**7**).

Table S12. Selected bond distances (Å) and bond angles (°) in **1**.

Table S13. Hydrogen bond table for **1** [Å and °].

Table S14. Selected bond distances (Å) and bond angles (°) in **2**.

Table S15. Hydrogen bond table for **2** [Å and °].

Table S16. Selected bond distances (Å) and bond angles (°) in **3**.

Table S17. Hydrogen bond table for **3** [Å and °].

Table S18. Selected bond distances (Å) and bond angles (°) in **4**.

Table S19. Hydrogen bond table for **4** [Å and °].

Table S20. Selected bond distances (Å) and bond angles (°) in **5**.

Table S21. Hydrogen bond table for **5** [Å and °].

Table S22. Selected bond distances (Å) and bond angles (°) in **6**.

Table S23. Hydrogen bond table for **6** [Å and °].

Table S24. Selected bond distances (Å) and bond angles (º) in **7**.

Table S25. Hydrogen bond table for **7** [Å and °].

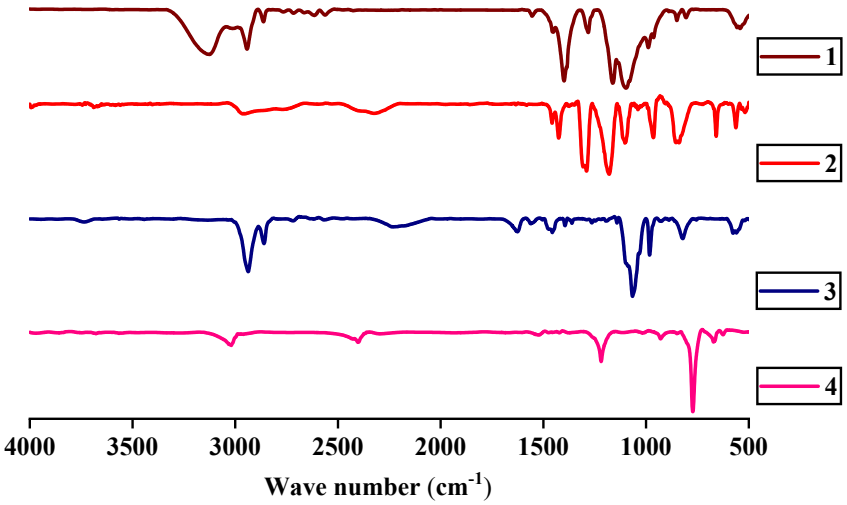

Figure S1. FT-IR spectra of compounds **1** and **3** (as KBr diluted discs), as well as **2** and **4** in the liquid state.

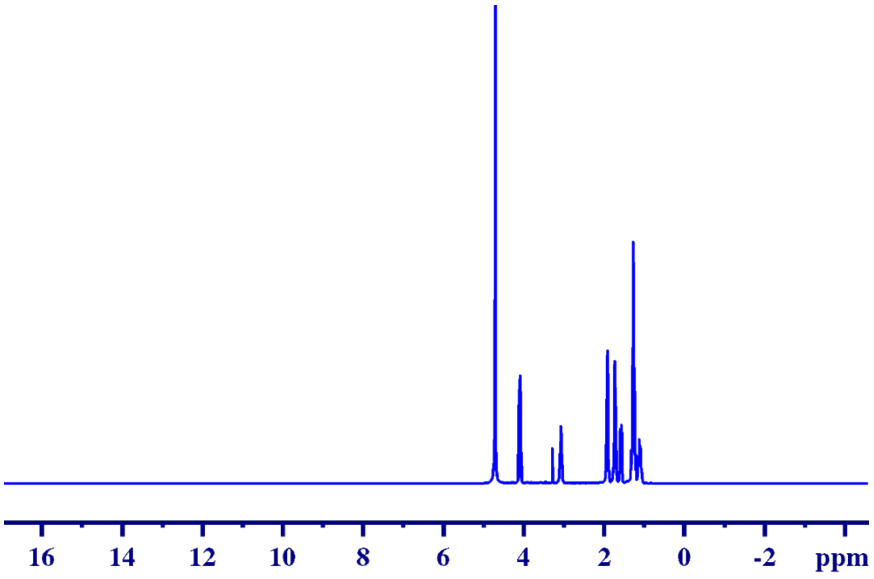

Figure S2. ^{1}H NMR spectrum of compound **1** in D_2O (400 MHz).

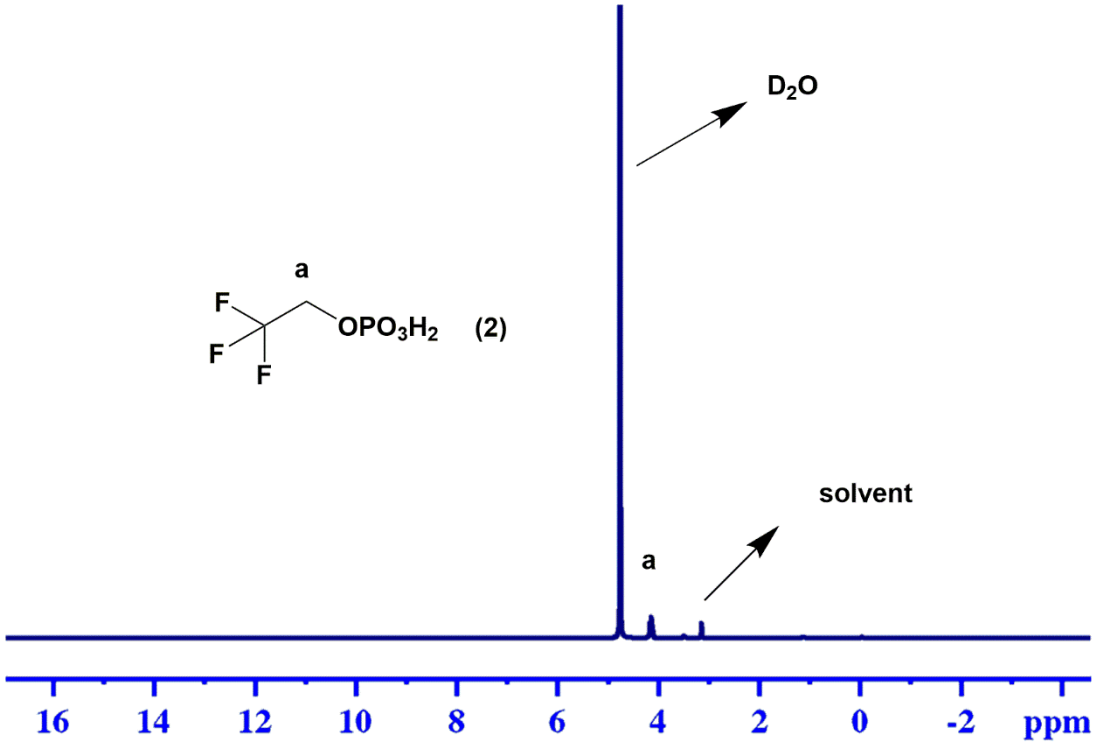

Figure S3. ^{1}H NMR spectrum of compound **2** in D_2O (400 MHz).

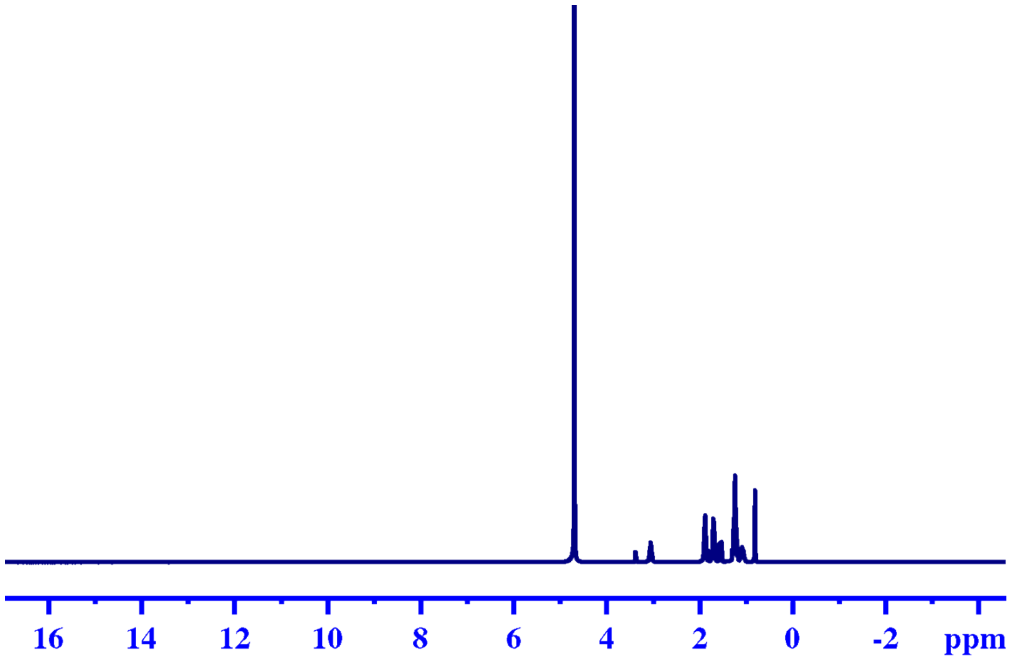

Figure S4. ^{1}H NMR spectrum of compound **3** in D_2O (400 MHz).

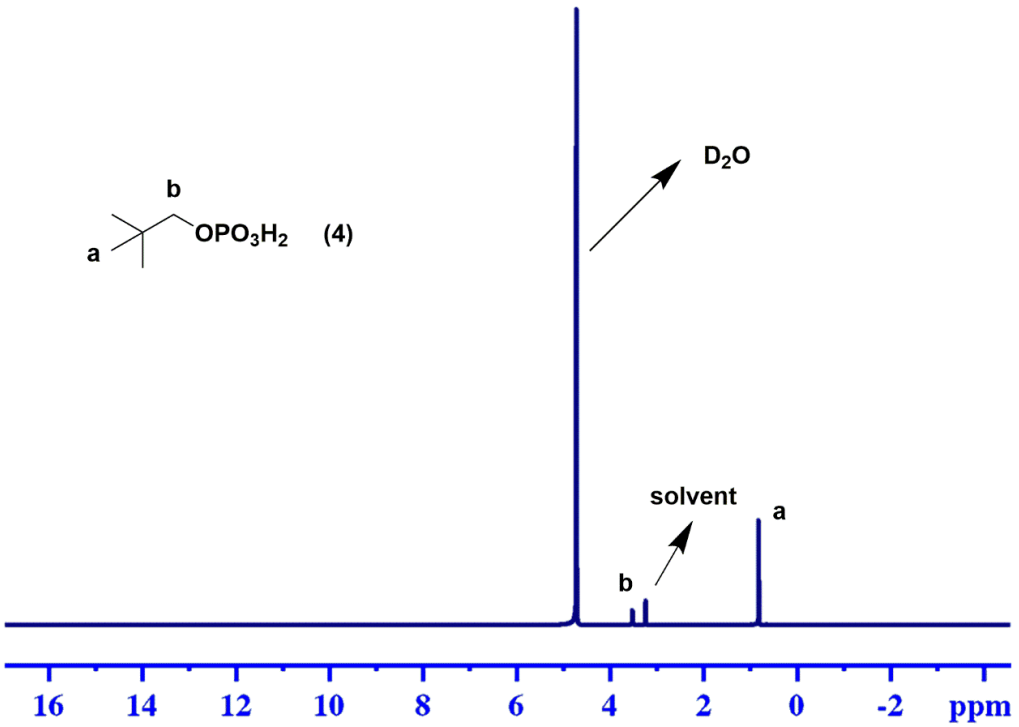

Figure S5. ^{1}H NMR spectrum of compound **4** in D_2O (400 MHz).

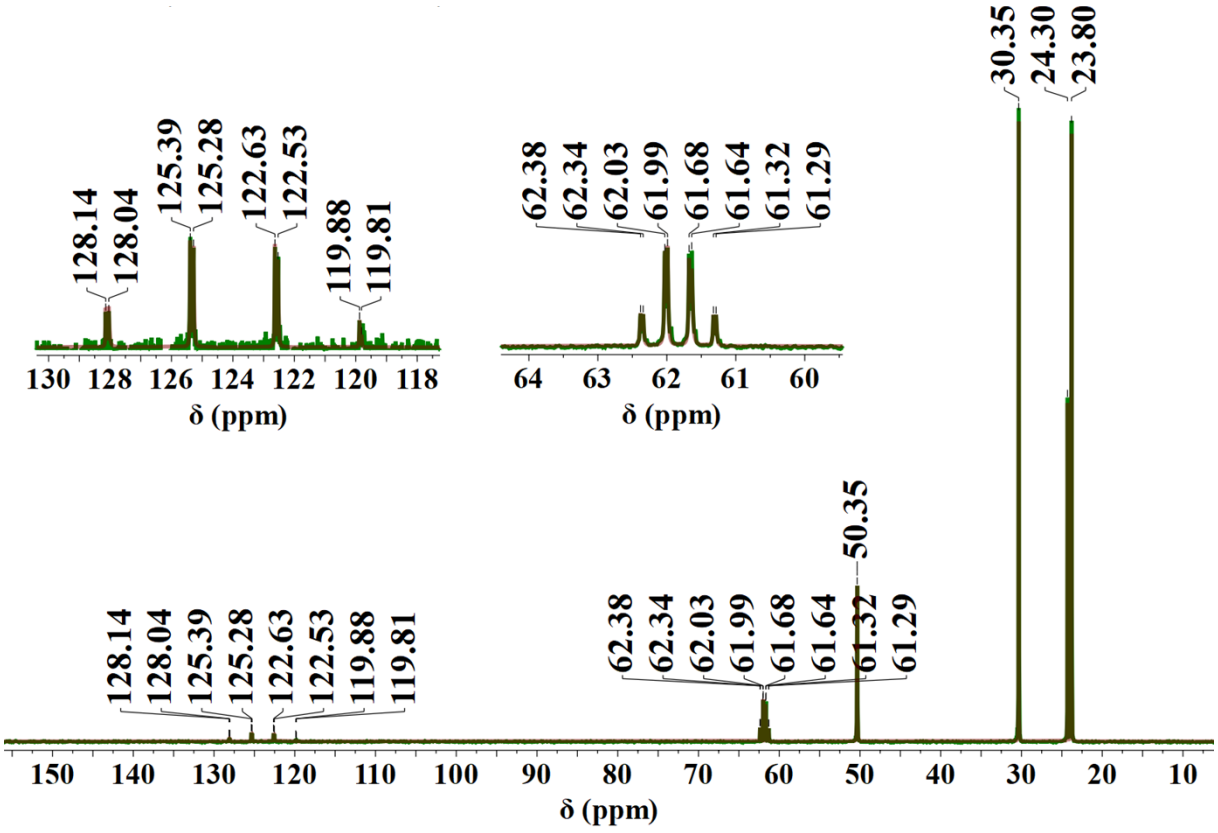

Figure S6. ^{13}C NMR spectrum of compound **1** in D_2O (101 MHz).

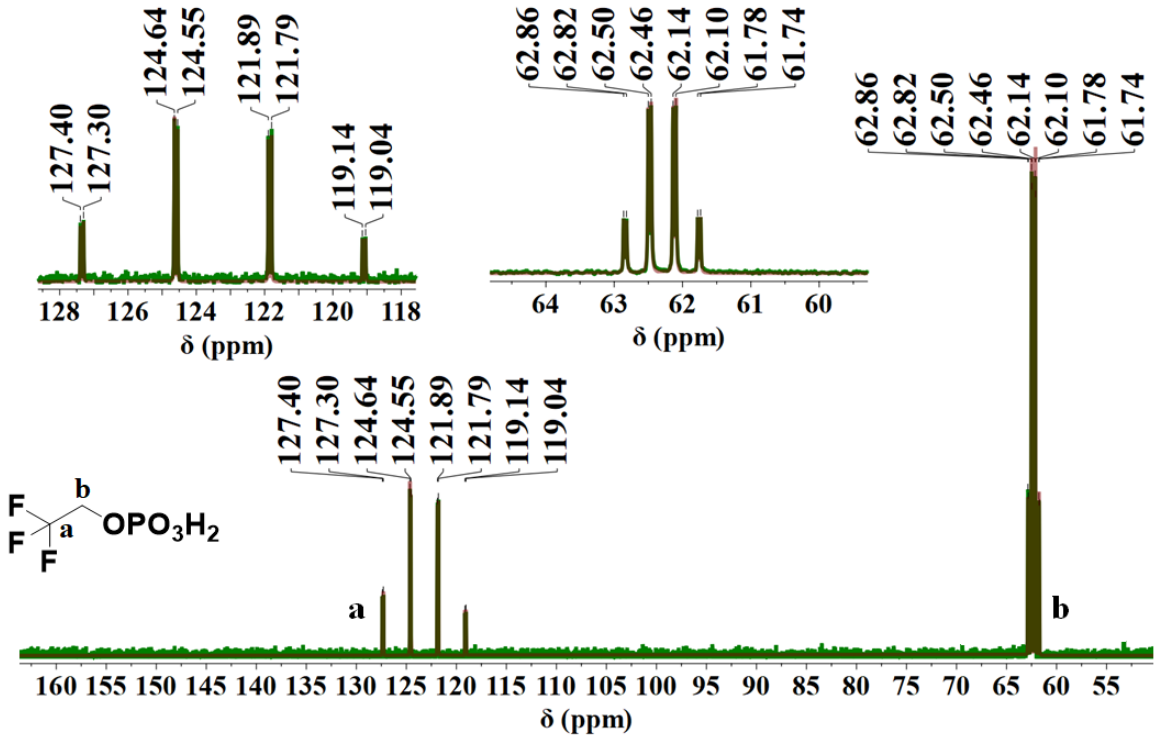

Figure S7. ^{13}C NMR spectrum of compound **2** in D_2O (101 MHz).

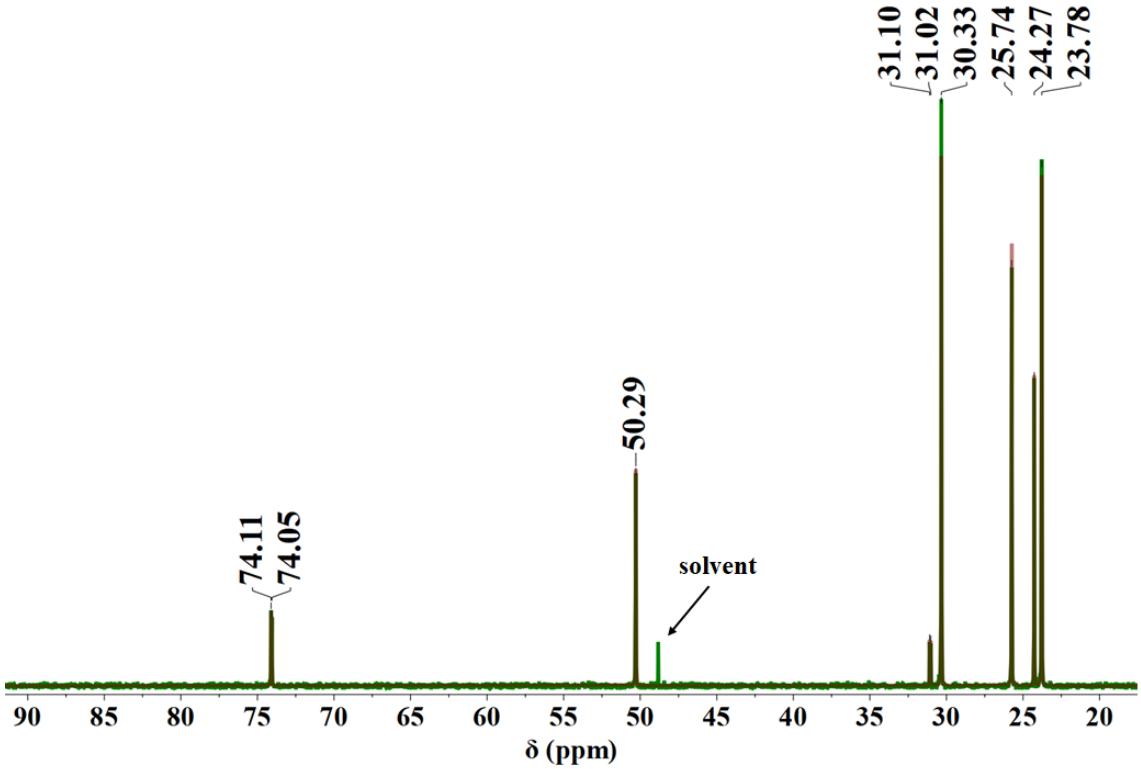

Figure S8. ^{13}C NMR spectrum of compound **3** in D_2O (101 MHz).

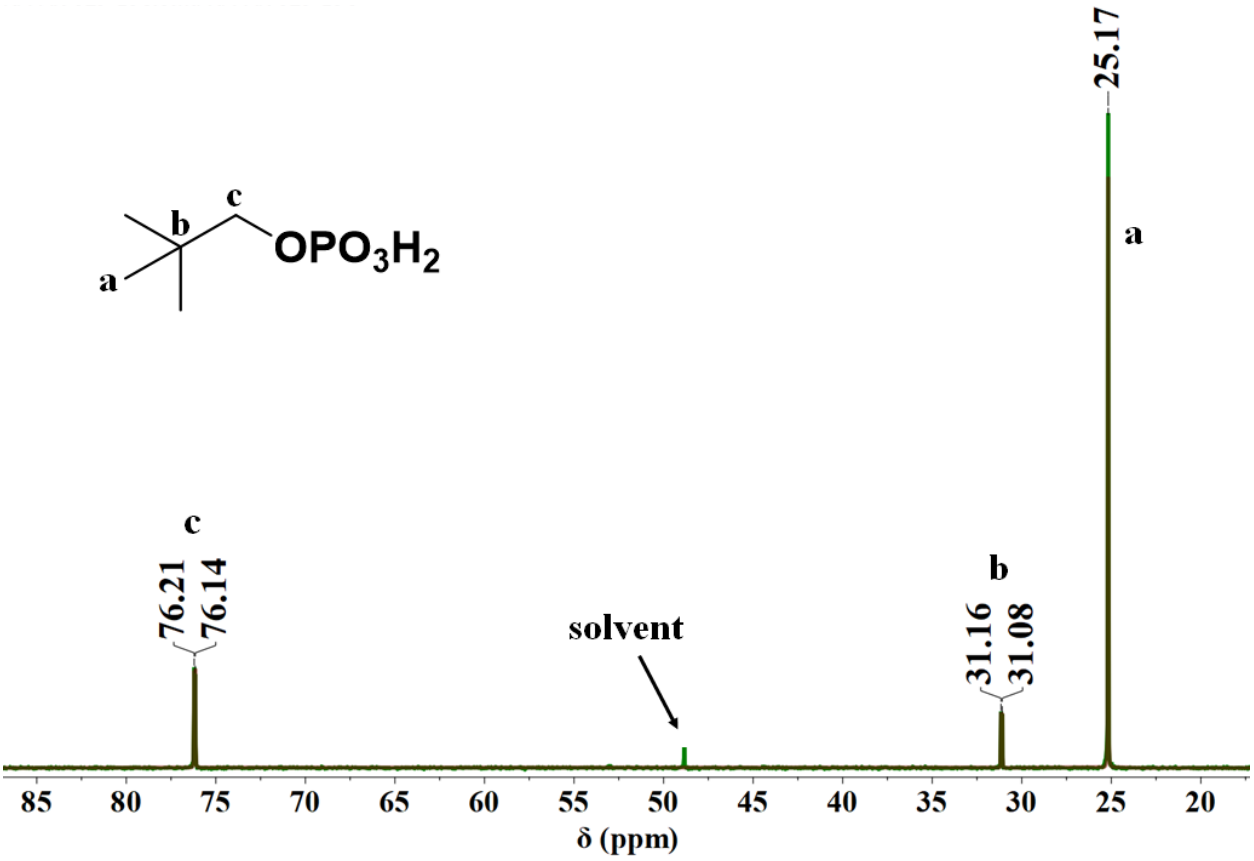

Figure S9. ^{13}C NMR spectrum of compound **4** in D_2O (101 MHz).

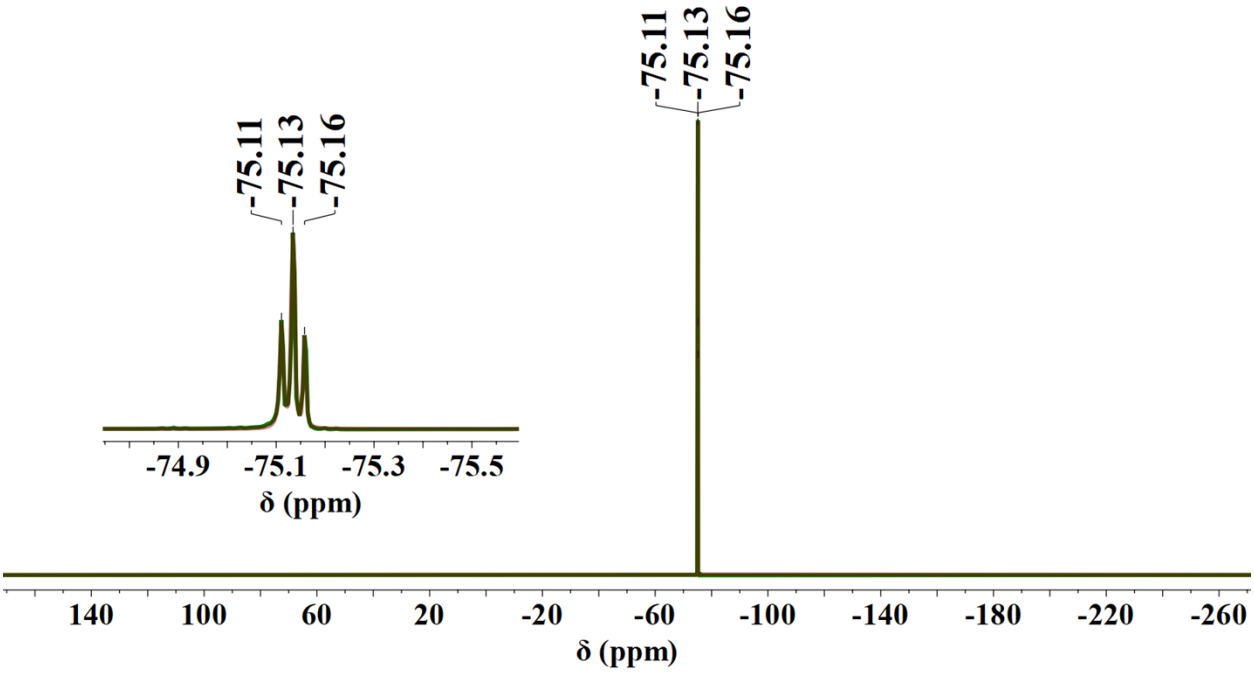

Figure S10. ^{19}F NMR spectrum of compound **1** in D_2O (376 MHz).

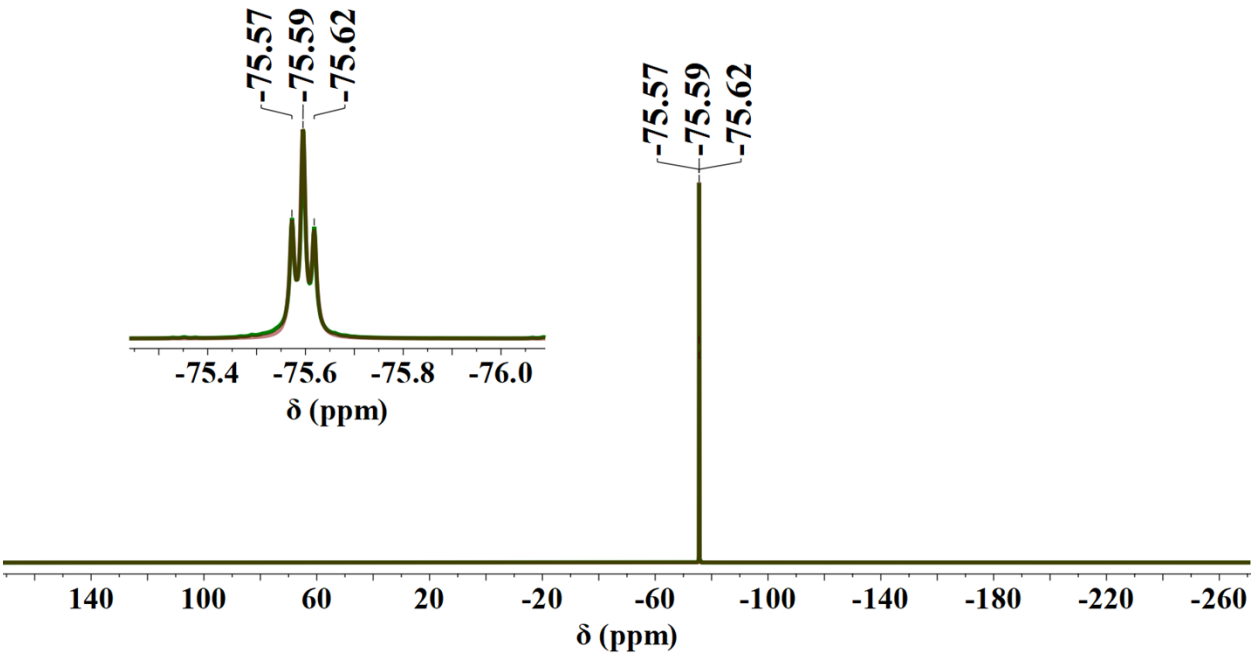

Figure S11. ^{19}F NMR spectrum of compound **2** in D_2O (376 MHz).

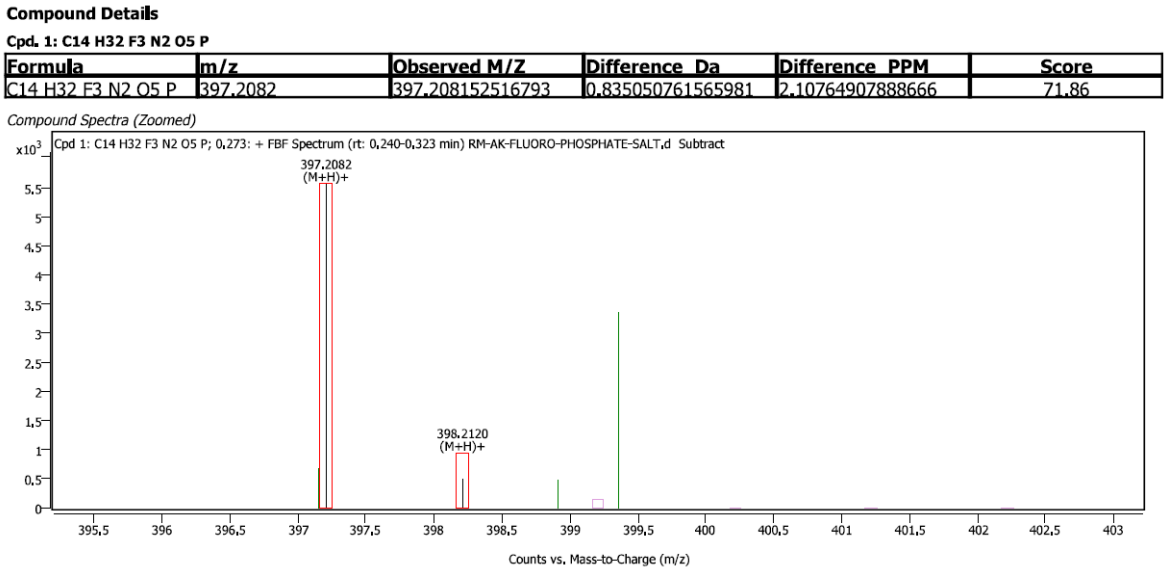

Figure S12. ESI-MS of compound $[CyNH_3]_2[(CF_3CH_2O)PO_3]\cdot H_2O$ **(1)** (in MeOH).

Compound Details

Cpd. 1: C18 H45 N2 O6 P

Formula	m/z	Observed M/Z	Difference_Da	Difference_PPM	Score
C18 H45 N2 O6 P	416.3010	416.301042743946	-0.439458620746791	-1.05562578024773	74.44

Compound Spectra (Zoomed)

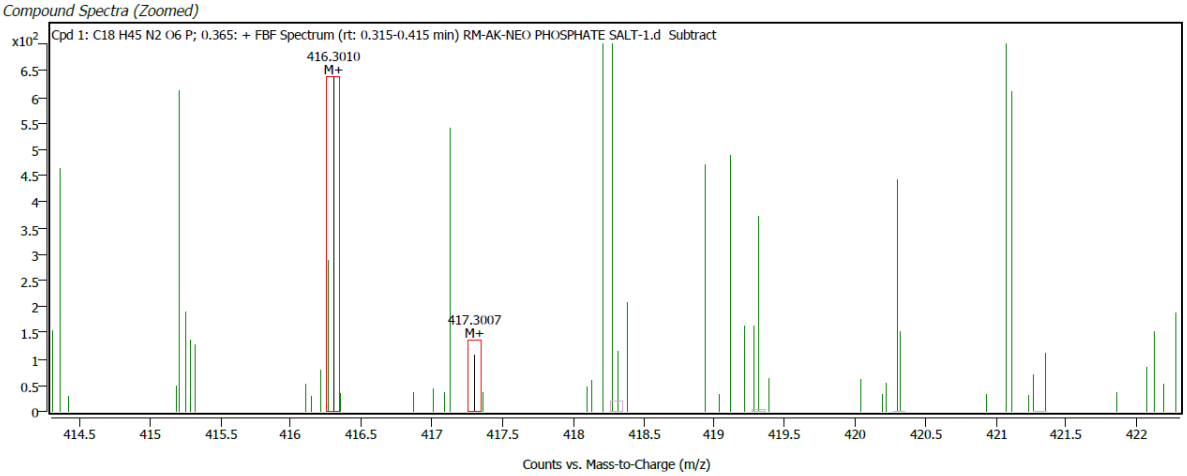

MassHunter Qual 10.0
(End of Report)

Figure S13. ESI-MS of compound $[CyNH_3]_2[((CH_3)_3CCH_2O)PO_3]\cdot H_2O\cdot MeOH$ **(3)** (in MeOH).

Compound Details

Cpd. 1: C2 H4 F3 O4 P

Formula	m/z	Observed M/Z	Difference_Da	Difference_PPM	Score
C2 H4 F3 O4 P	180.9871	180.987051590673	-0.154142413748559	-0.85644223775211	85.61

Compound Spectra (Zoomed)

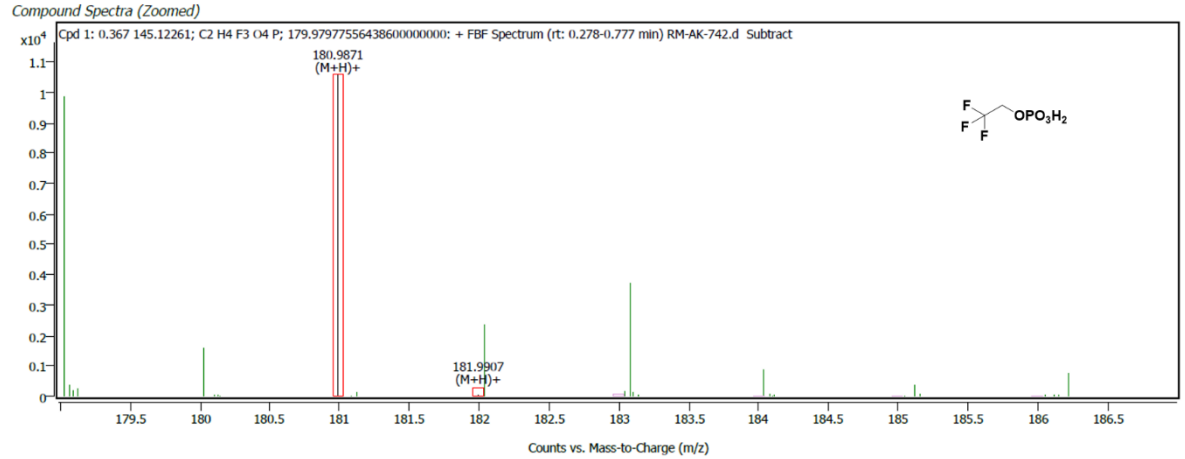

MassHunter Qual 10.0
(End of Report)

Figure S14. ESI-MS of compound $CF_3CH_2OPO_3H_2$ **2** (in MeOH).

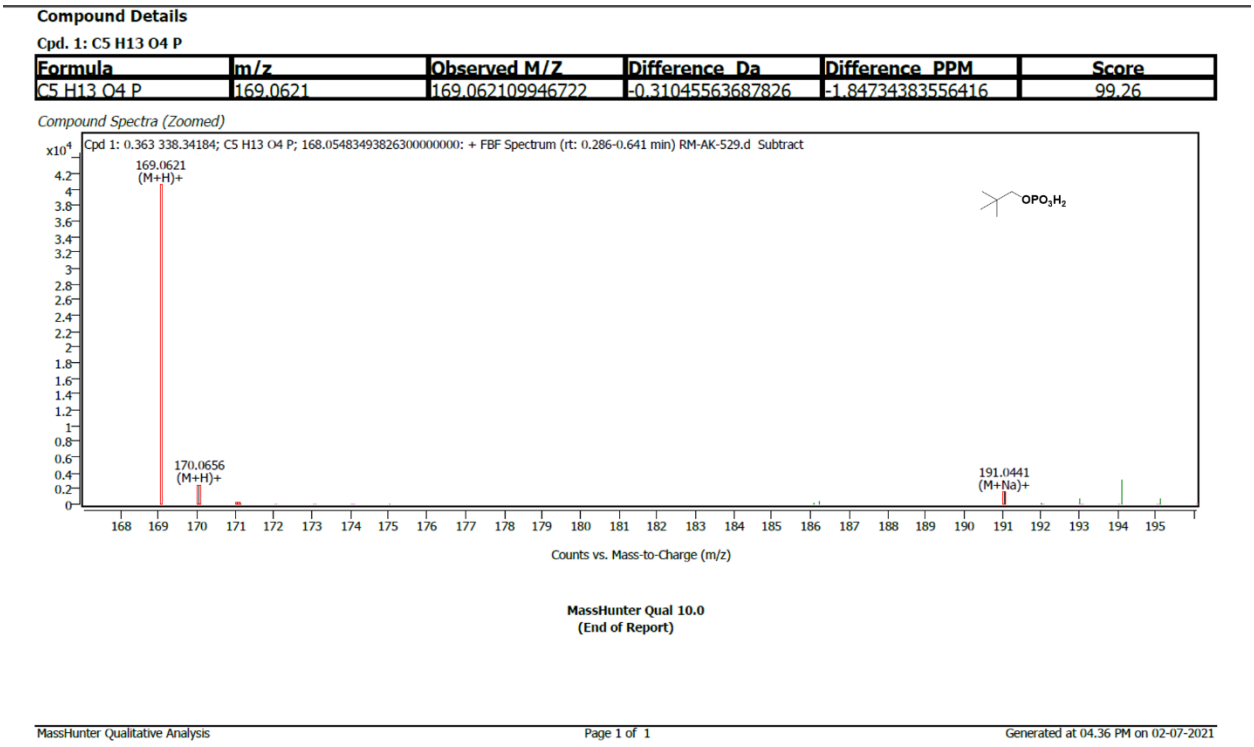

Figure S15. ESI-MS of compound $(CH_3)_3CCH_2OPO_3H_2$ **4** (in MeOH).

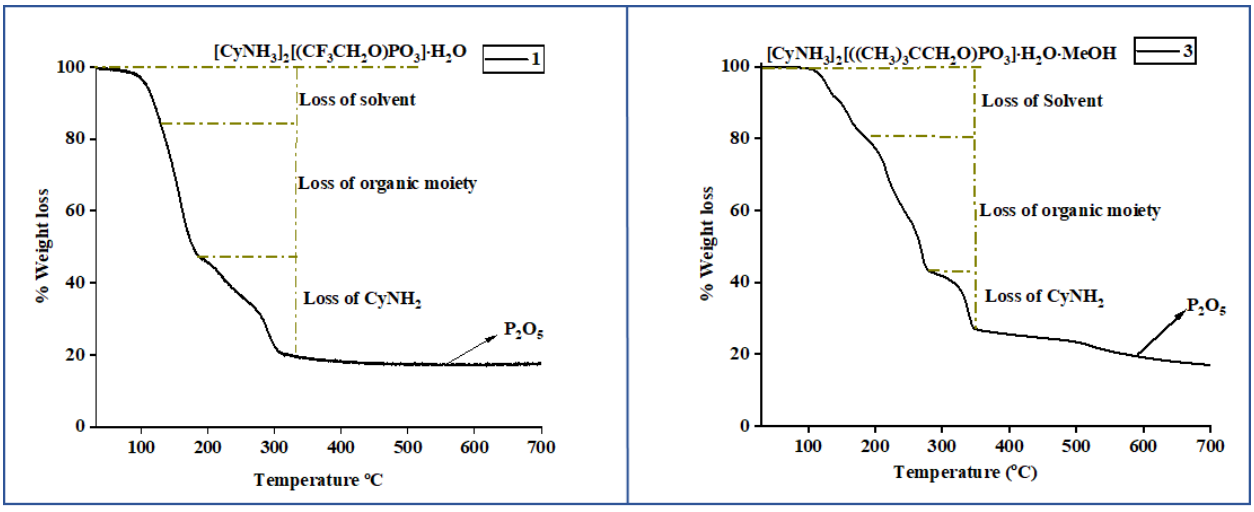

Figure S16. TGA profiles for compounds **1** and **3**.

Hirshfeld surface analysis

Crystal Explorer 17.5[1] was used to create a Hirshfeld surface (HS) analysis and their corresponding 2D fingerprint plots for compounds **2** and **4** in order to visualize the intermolecular interactions in the crystal of the title compounds.[2, 3] The normalized contact distance (d_{norm}), which is determined using Equation **(1)**, is used to map the Hirshfeld surface.

$$d_norm = \frac{d_i - r_i^v dw}{r_i^v dw} + \frac{d_e - r_e^v dw}{r_e^v dw}$$

Equation **(1)**,

The molecular packing in crystals is mostly caused by tight intermolecular interactions, which are identified using the 3D d_{norm} surface. It is possible to describe the intermolecular interaction in the crystal using the sign of d_{norm}. Intermolecular contacts are referred to as near molecular interactions when $d_{norm} < 0$ and they are less than van der Waals radii. Intermolecular contacts are longer than van der Waals radii when $d_{norm} > 0$, and they are similar to van der Waals radii when $d_{norm} = 0$. On the Hirshfeld surfaces, these three intermolecular interactions can be distinguished by their colour. The red region indicates short interactions, the blue area represents long contacts, and the white area shows contacts with lengths equal to the total of the participating atoms van der Waals radii. Using the Crystal Explorer 17.5 software,[1] the Hirshfeld surfaces and the associated 2D fingerprint plots were created. With the use of d_{norm} (normalized contact distance) and 2D fingerprint plots, the quantification and decoding of the intermolecular interactions in the crystal packing are respectively displayed. Short interatomic contacts give rise to the dark-red spots on the d_{norm} surface, whereas other intermolecular interactions result in light-red spots. The color gradient (blue to red) in the fingerprint plots represents the relative contribution of the contacts over the surface. The (Figure 17) shows the Hirshfeld surface plotted across d_{norm} in the range of -0.6990 to 1.1557 a.u for compound **2** and from -0.7679 to 1.3087 a.u. for compound **4**. Table S1 and S2, provides information about the intermolecular interactions for both of the compounds, which are depicted as spots on the Hirshfeld surface. Therefore, the primary interactions in both the compounds (**2** and **4**) that contribute to the molecular packing in the crystal are O-H interactions. Additional chemical insight into molecular packing is provided by Koendrink[4] with helpful metrics of curvedness (Figure 18), shape-index (Figure 19), and fragment patches (Figure 20). The first one, de, represents the distance to the closest external nucleus from the point (Figure 21), while the second one, di, represents the distance to the closest internal nucleus from the point (Figure 22).

Low surface curvature indicates a flat area and maybe a hint of π…π stacking in the crystal. The absence of stacking is shown by a Hirshfeld surface with strong curvedness, which is accentuated by dark-blue edges. The shape index, a qualitative measure of shape, is perceptive to minute variations in surface shape, especially when applied to flat areas. The complementing "bumps and hollows" are represented by two shape indices with significant differences. The donor of an intermolecular connection is shown by the blue bump-shape and shape-index > 1, and the acceptor is shown by the red hollow and shape-index < 1.

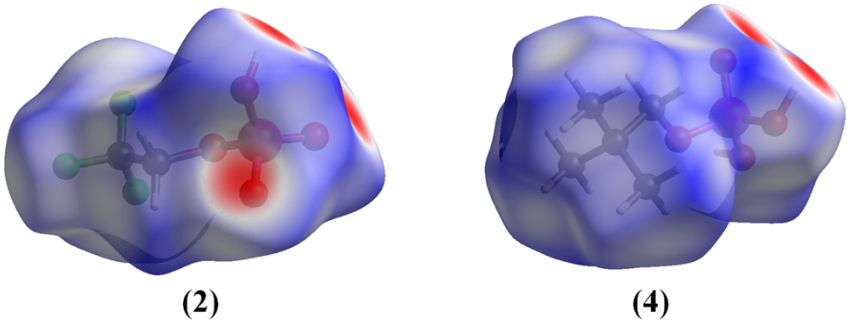

(2) **(4)**

Figure S17. Hirshfeld Surfaces (d_{norm}) of compounds 2 and 4.

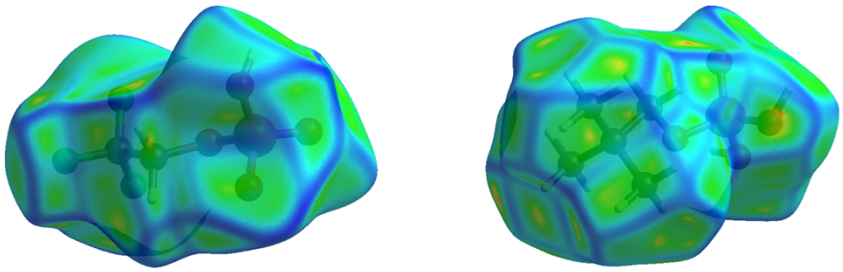

(2) **(4)**

Figure S18. Hirshfeld Surfaces (Curvedness) of compounds 2 and 4.

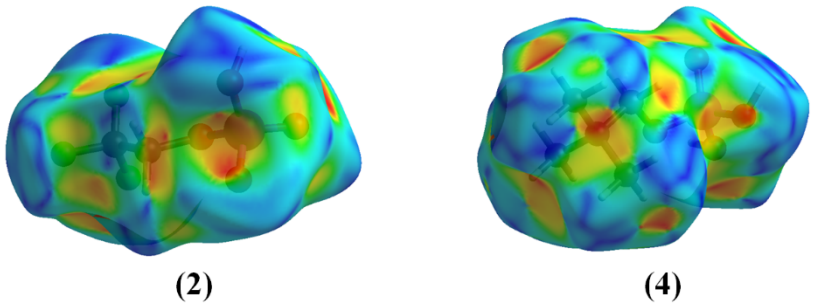

(2) (4)

Figure S19. Hirshfeld Surfaces (Shape Index) of compounds 2 and 4.

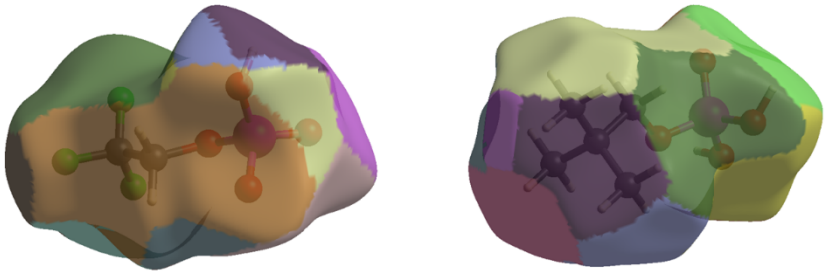

(2) (4)

Figure S20. Hirshfeld Surfaces (Fragment Patches) of compounds 2 and 4.

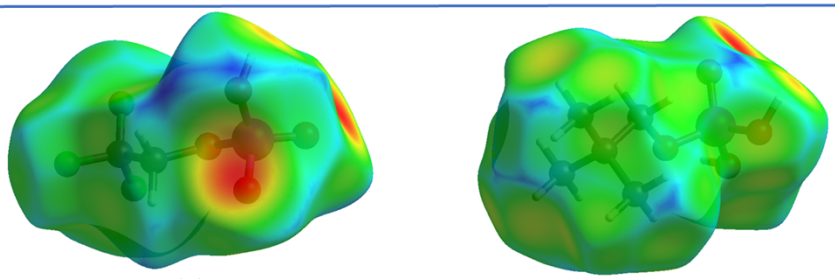

(2) (4)

Figure S21. Hirshfeld Surfaces (d_e) of compounds 2 and 4.

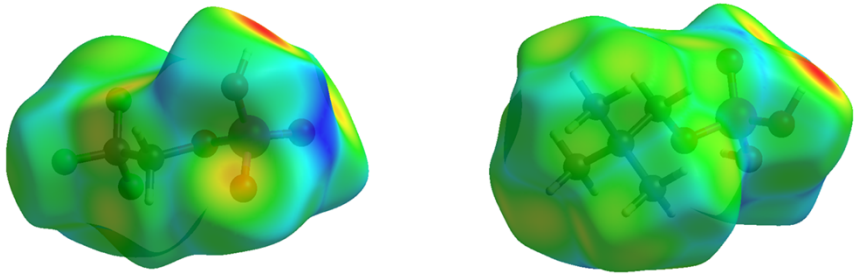

(2) (4)

Figure S22. Hirshfeld Surfaces (d_i) of compounds 2 and 4.

Two-dimensional (2D) fingerprint plots from Hirshfeld surface analyses for the compounds **2** and **4** are depicted in (Figures S23† and S24†), respectively, which also shows the relative percentage contribution of the compound key intermolecular interactions. Tables S3 and S4 provide details about the intermolecular interactions of both of the compounds, which are depicted as spots on the Hirshfeld surface in (Figures S23† and S24†). By quantitatively describing the nature and kind of intermolecular interactions, the 2D Fingerprint plots complement the Hirshfeld surface. The most significant interaction in compound **2** is O---H/H---O, with the contribution of 40% to the total crystal packing. Additionally, the FP plots for H---F/F---H (22.8%), F---F (19.4%), F---O/O---F (8.4%), O---O (5.6%), and H---H (3.8%) disclose details about the intermolecular hydrogen bonds and their distinct contributions to crystal packing. Whereas, the 2D fingerprint plots for compound **4** with overall Hirshfeld surfaces of (19.3 + 15.9 = 35.2%) showed the O---H interactions as scattered spikes. The contribution from the H—H contacts is seen between the pair of sharp spikes of O–H and is characterized by significant hydrogen-bonding interactions (61.1%). While the other fingerprint plots are also shown in (Figure S24†).

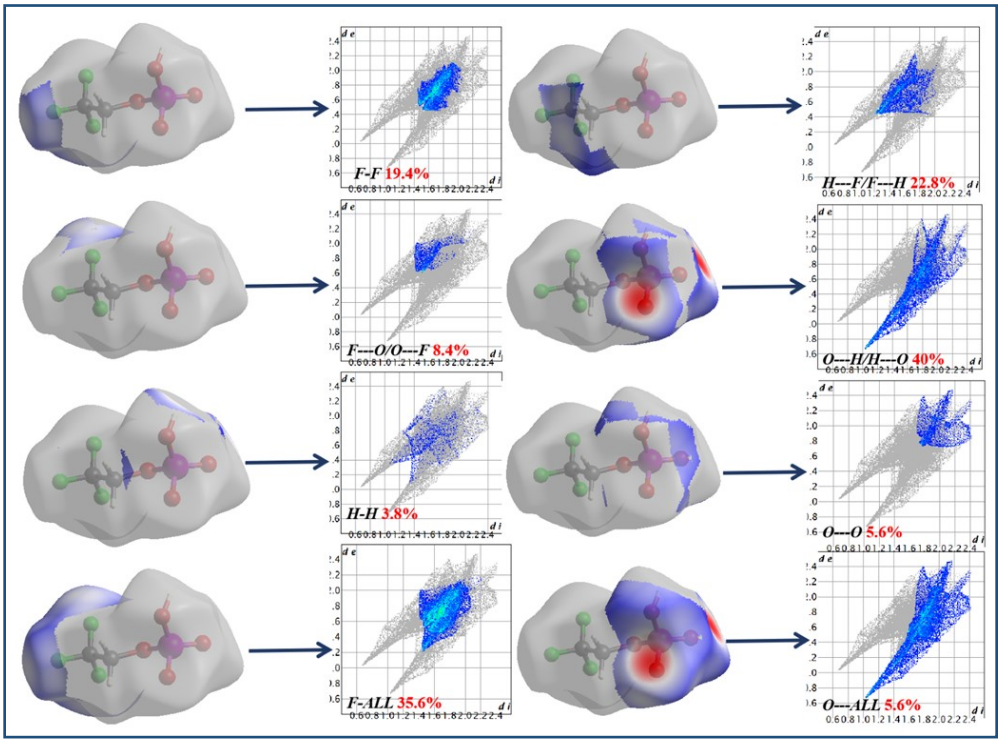

Figure S23: (2D) fingerprint plots from Hirshfeld surface analyses for compound **2**.

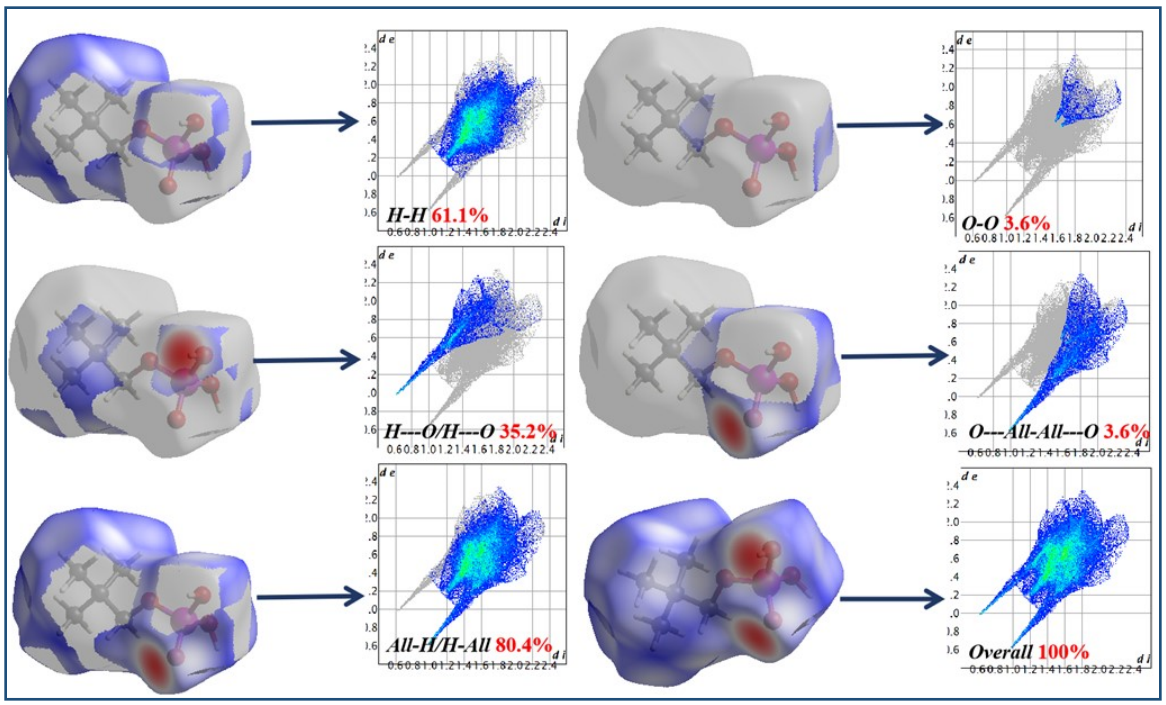

Figure S24: (2D) fingerprint plots from Hirshfeld surface analyses for compound **4**.

Table S1: Surface property information in Hirshfeld for compound 2.

Mode	Minimum interaction	Mean interaction	Maximum interaction
dnorm	-0.6990	0.3762	1.1557
di	0.6749	1.6549	2.4235
de	0.6758	1.6817	2.4975
Shape Index	-0.9934	0.2914	0.9964
curvedness	-3.8549	-0.9018	0.2557
Fragment patches	0	6.5783	15.0000

Table S2: Surface property information in Hirshfeld for compound **4**.

Mode	Minimum interaction	Mean interaction	Maximum interaction
dnorm	-0.7679	0.4993	1.3087
di	0.6307	1.5643	2.3670
de	0.6324	1.5903	2.3858

Shape Index	-0.9992	0.2792	0.9968
curvedness	-3.8524	-0.9377	0.3564
Fragment patches	0.0000	6.8468	13.0000

Table S3: Fingerprint percentage of the total surface area for closed contact between atoms inside and outside the surface for compound **2**.

Atoms Surface %	**P**	**F**	**O**	**H**	**C**	**All**
P	0	0	0	0	0	0
F	0	19.4	4.1	12.1	-	35.6
O	0	4.3	5.6	21.5	0	31.4
H	0	10.7	18.5	3.8	0	33.0
C	0	0	0	0	0	0
All	0	34.4	28.2	37.4	0	100

Table S4: Fingerprint percentage of the total surface area for closed contact between atoms inside and outside the surface for compound **4**.

Atoms Surface %	**P**	**O**	**H**	**C**	**All**
P	0	0	0	0	0
O	0	3.6	19.3	0	22.9
H	0	15.9	61.1	0	77.1
C	0	0	0	0	0
All	0	19.6	80.4	0	100

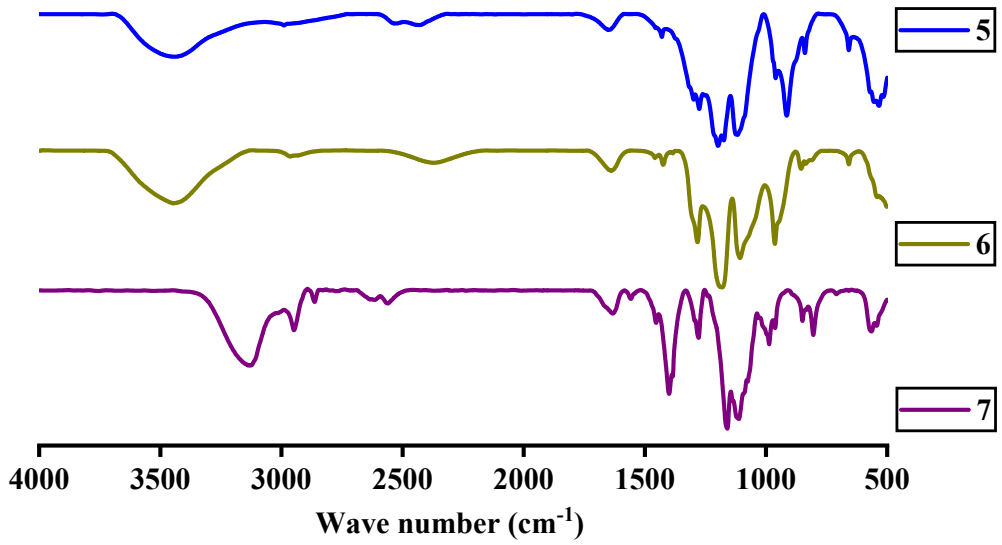

Figure S25. FT-IR spectra of compounds **5-7** as KBr diluted discs (as KBr diluted discs).

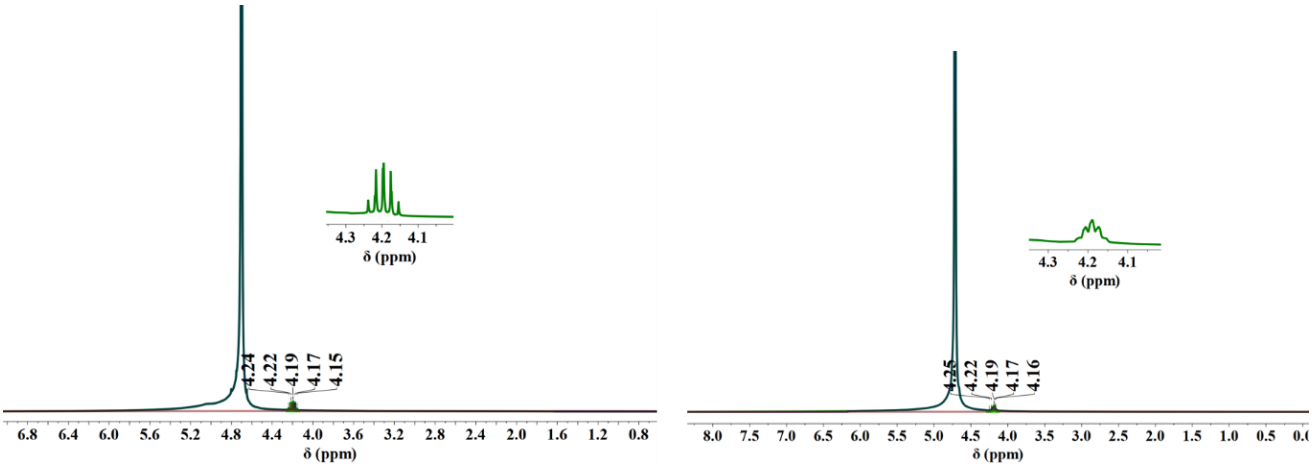

Figure S26. ^{1}H NMR spectra of compounds $[(CF_3CH_2PO_4HLi)_3]_n$ (**5**), (Left) and $[(CF_3CH_2PO_4HNa)_2]_n$ (**6**) (Right) in D_2O (400 MHz).

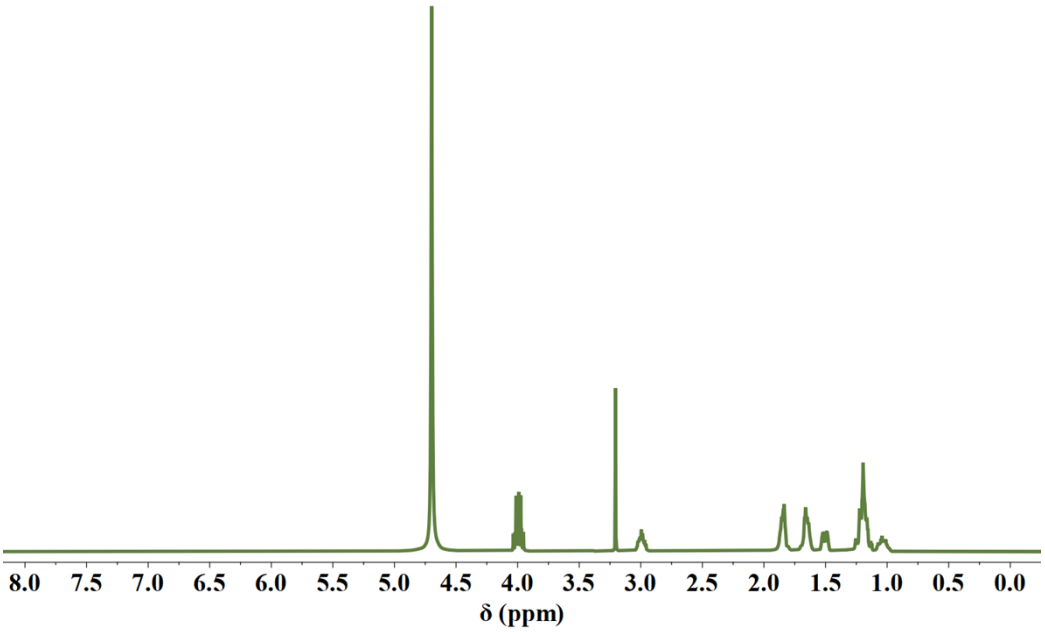

Figure S27. ^{1}H NMR spectrum of compound $[CF_3CH_2OPO_3(Na_{0.5})_2)(CyNH_3)\cdot(H_2O)_6]_n$ (**7**) in D_2O (400 MHz).

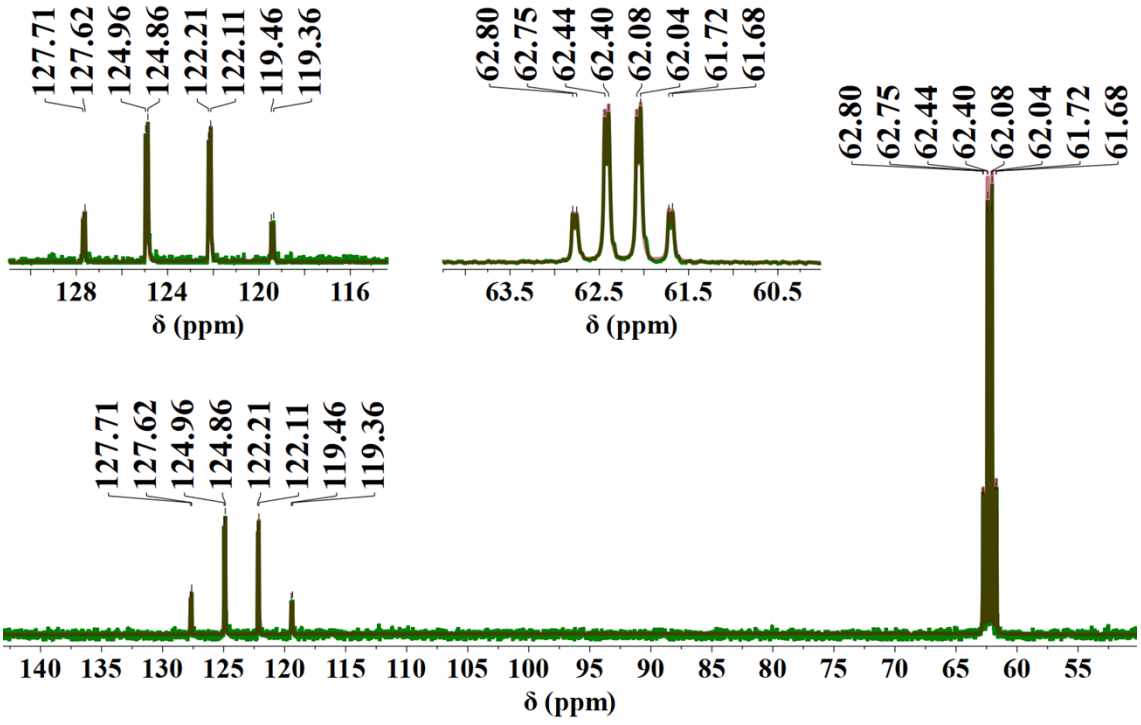

Figure S28. ^{13}C NMR spectrum of compound $[(CF_3CH_2PO_4HLi)_3]_n$ (**5**) in D_2O (101 MHz).

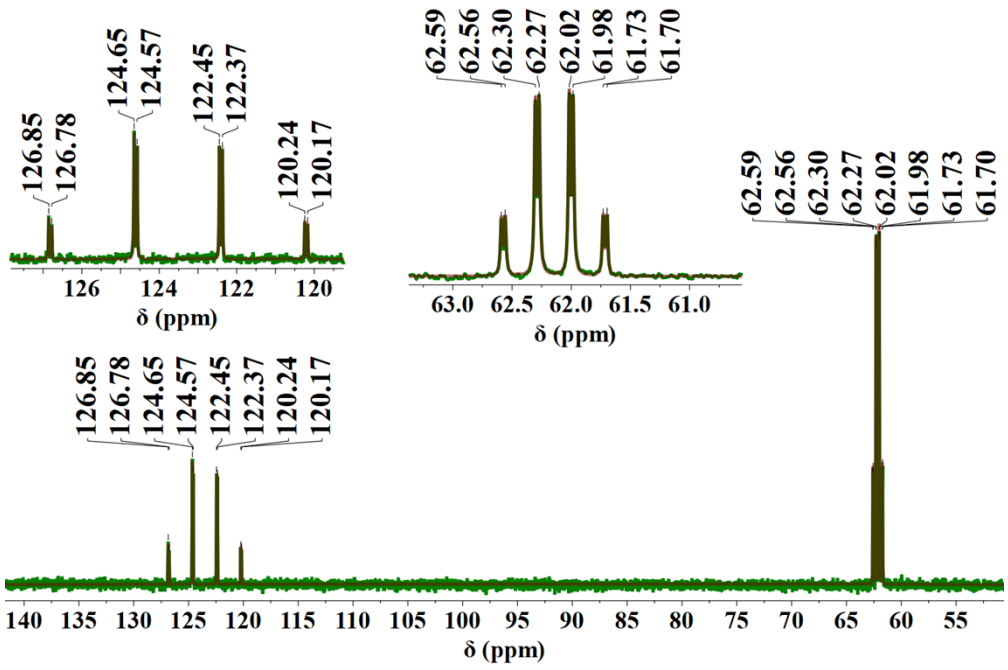

Figure S29. ^{13}C NMR spectrum of compound $[(CF_3CH_2PO_4HNa)_2]_n$ (**6**) in D_2O (125 MHz).

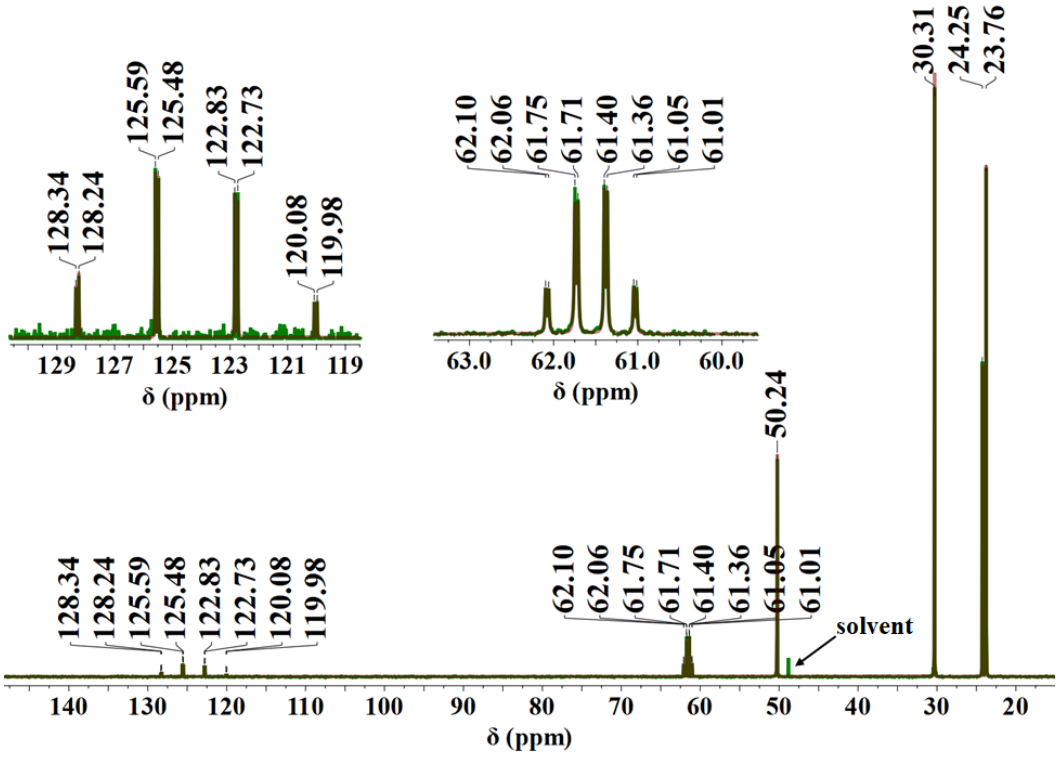

Figure S30. ^{13}C NMR spectrum of compound $[CF_3CH_2OPO_3(Na_{0.5})_2(CyNH_3)\cdot(H_2O)_6]_n$ (**7**) in D_2O (101 MHz).

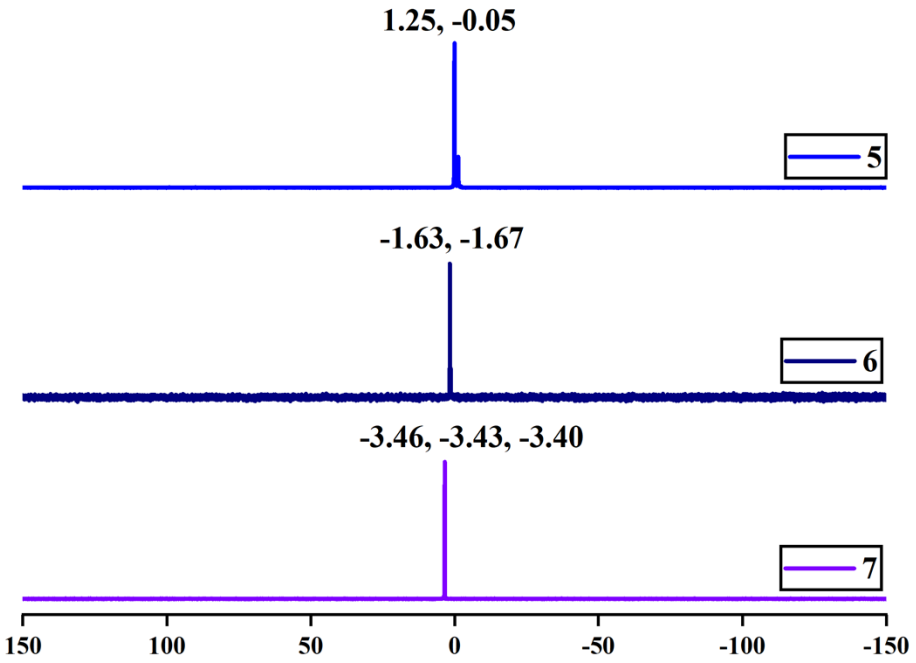

Figure S31. ^{31}P NMR spectra of compounds **5** (202 MHz), **6**, and **7** (162 MHz) in (CD_3OD).

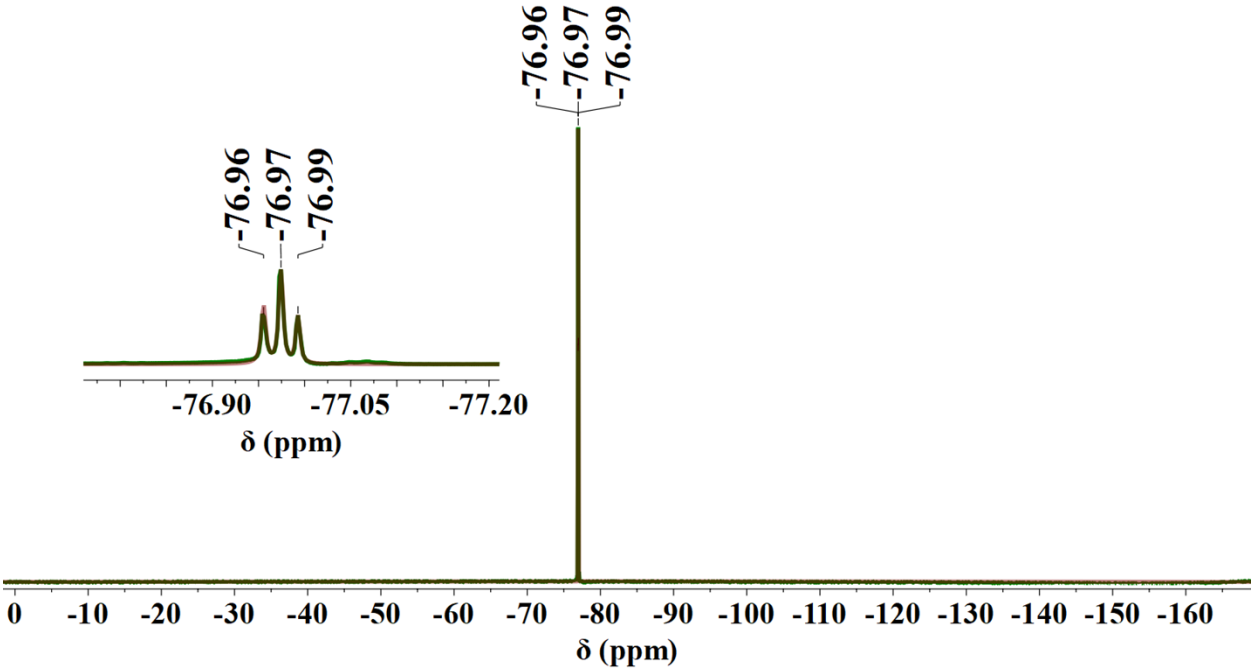

Figure S32. ^{19}F NMR spectrum of compound **5** (470 MHz) in (CD_3OD).

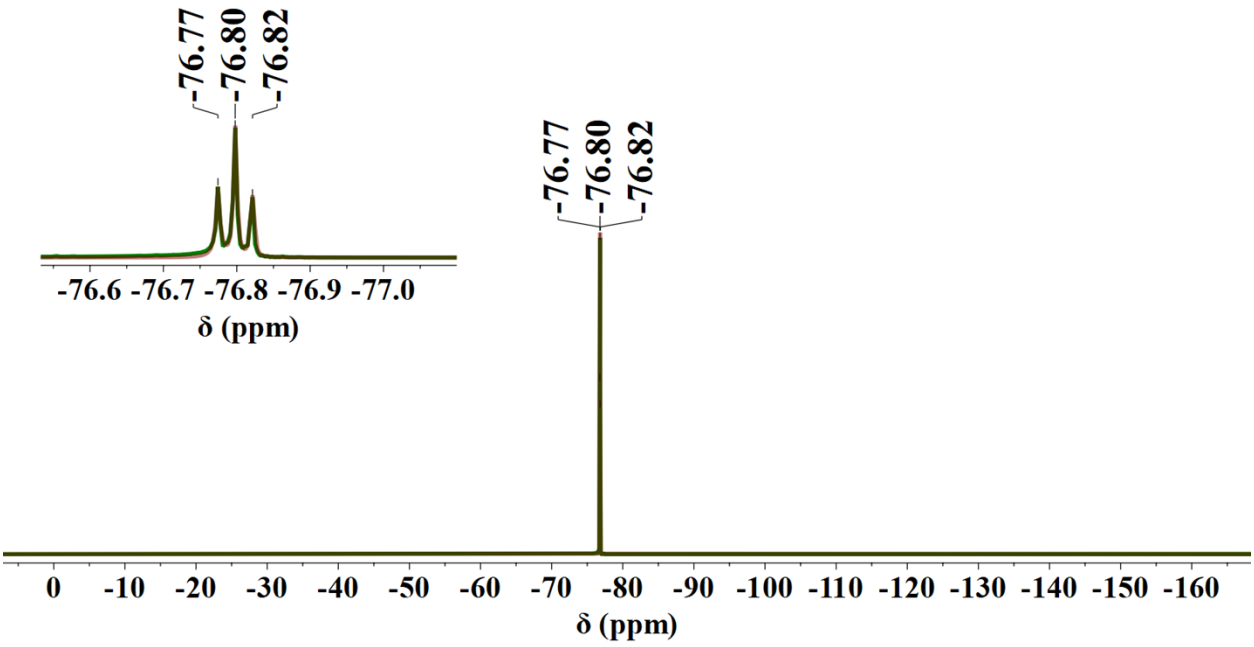

Figure S33. ^{19}F NMR spectrum of compound **6** (376 MHz) in (CD_3OD).

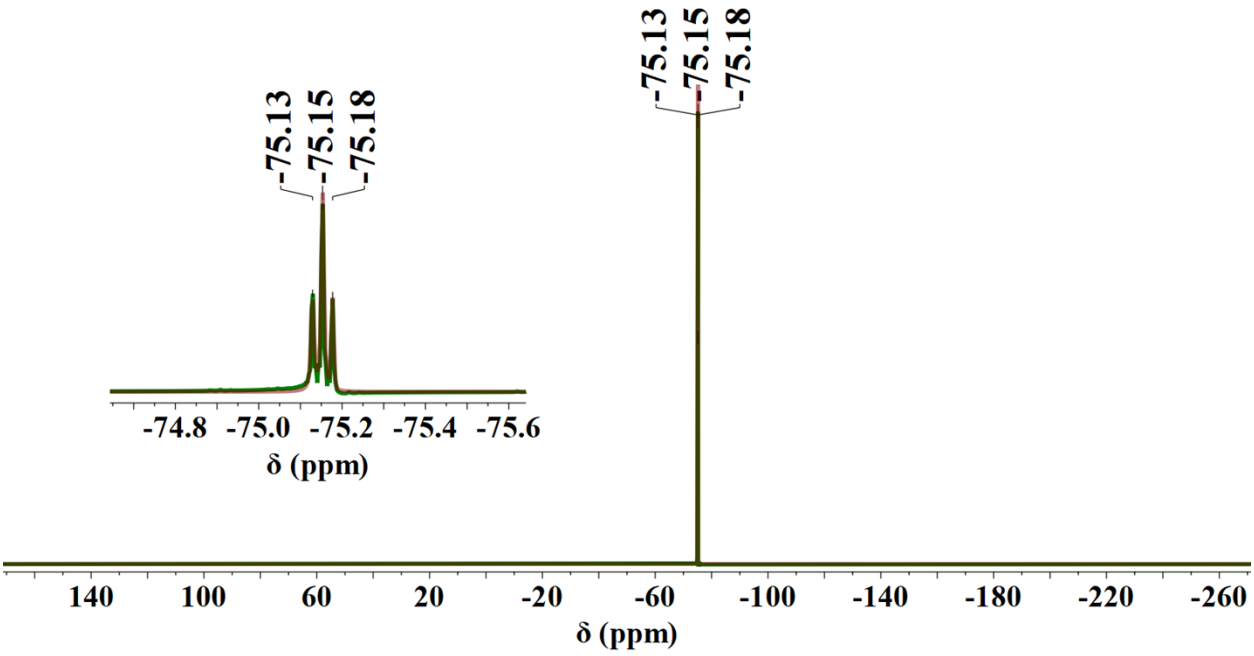

Figure S34. ^{19}F NMR spectrum of compound **7** (470 MHz), in (CD_3OD).

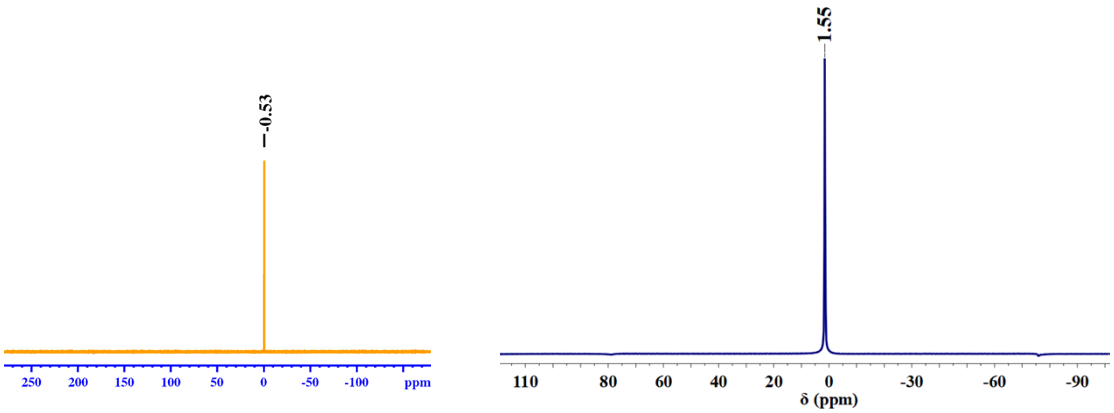

Figure S35. ^{7}Li NMR spectra of compounds $[(CF_3CH_2PO_4HLi)_3]_n$ (**5**) (194 MHz) in (CD_3OD) (Left) and CP-MAS ^{7}Li NMR spectra (233 MHz) (Right).

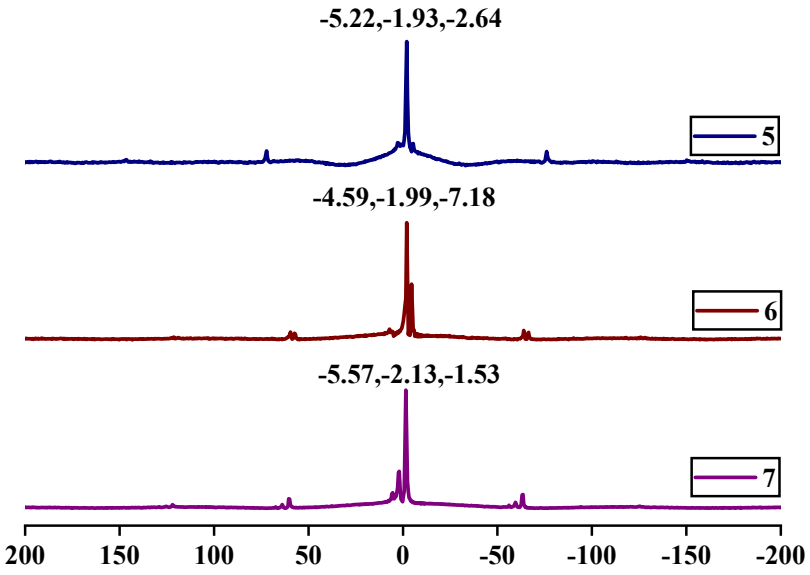

Figure S36. The CP-MAS ^{31}P NMR spectra of compounds **5**–**7**.

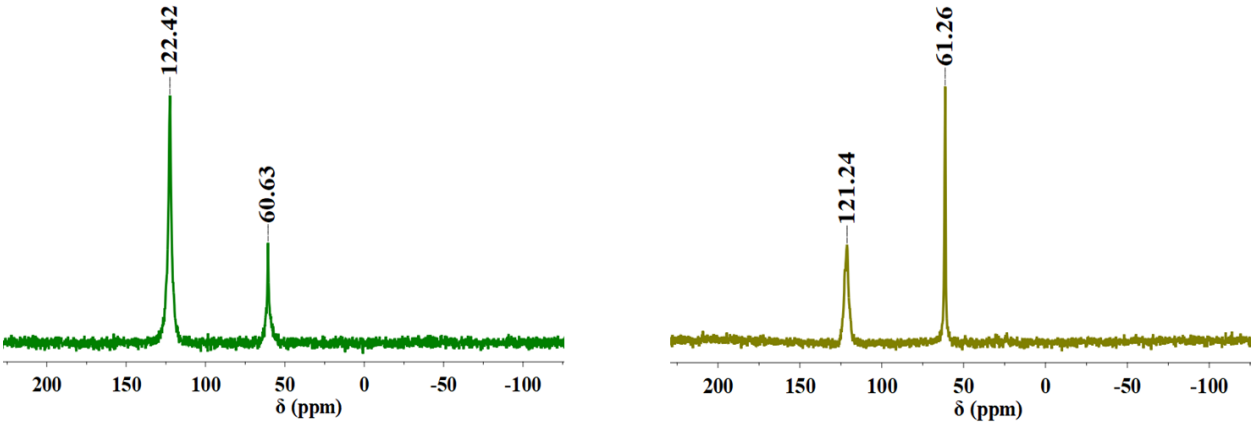

Figure S37. The CP-MAS ^{13}C NMR spectra (150 MHz) of compounds $[(CF_3CH_2PO_4HLi)_3]_n$ (**5**); (left), and $[(CF_3CH_2PO_4HNa)_2]_n$ (**6**); (right).

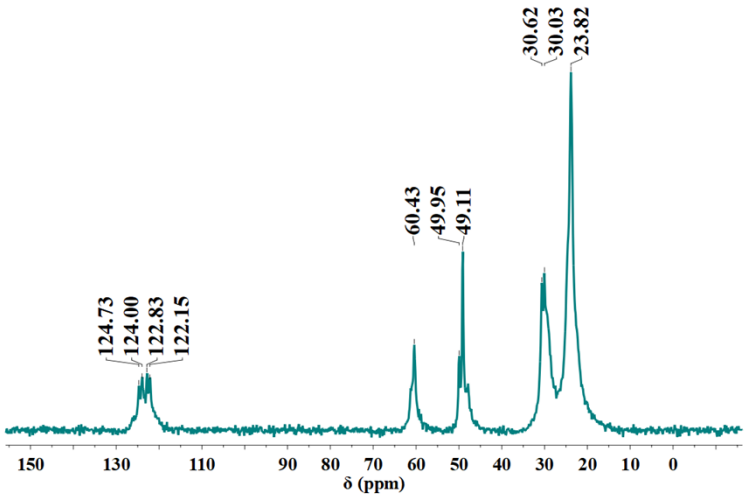

Figure S38. The CP-MAS ^{13}C NMR spectrum (150 MHz) of $[CF_3CH_2OPO_3(Na_{0.5})_2(CyNH_3)\cdot(H_2O)_6]_n$ (**7**).

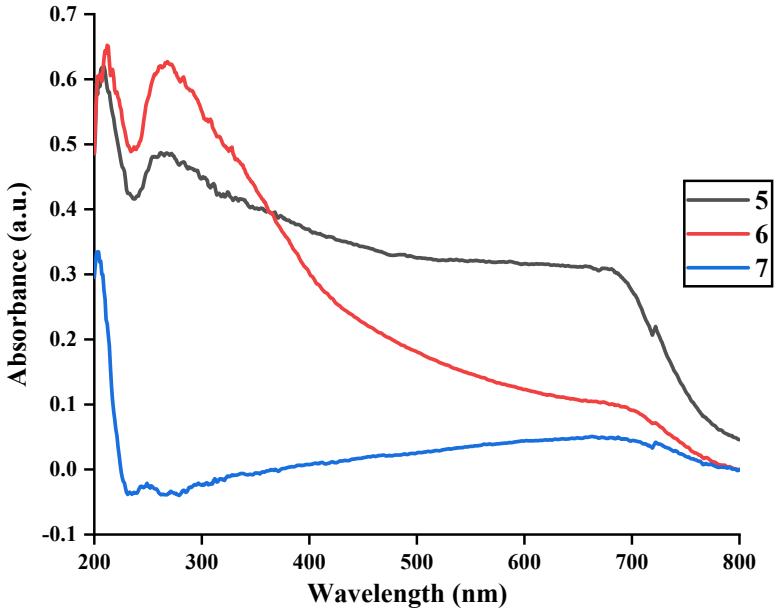

Figure S39. DR-UV-Vis spectra of compounds **5–7**.

SHAPE analysis of alkali metals centers in 5-7

Continuous Shape measurements reveal that the core geometries of the alkali metal center in all three complexes (**5-7**) differ, with minimal deviation from ideal T_d symmetry in compound **5**, D_{3h} symmetry in compound **6**, and similarly O_h symmetry in compound **7**.

Table S5. Shape analysis in complex 5 (Li1 atom)

Structure	SP-4	**T-4**	SS-4	vTBPY-4
Shape	Square	**Tetrahedron**	Seesaw	Vacant trigonal bipyramid
Symmetry	D_{4h}	***Td***	C_{2v}	C_{3v}
Deviation	30.849	**0.484**	7.476	3.115

Table S6. Shape analysis in complex **5** (Li2 atom)

Structure	SP-4	**T-4**	SS-4	vTBPY-4
Shape	Square	**Tetrahedron**	Seesaw	Vacant trigonal

				bipyramid
Symmetry	D_{4h}	***Td***	C_{2v}	C_{3v}
Deviation	28.928	**0.383**	8.086	3.106

Table S7. Shape analysis in complex **5** (Li3 atom)

Structure	SP-4	**T-4**	SS-4	vTBPY-4
Shape	Square	**Tetrahedron**	Seesaw	Vacant trigonal bipyramid
Symmetry	D_{4h}	***Td***	C_{2v}	C_{3v}
Deviation	27.339	**1.155**	7.500	2.855

Table S8. Shape analysis in complex **6** (Na1 atom)

Structure	HP-6	PPY-6	**OC-6**	**TPR-6**	JPPY-6
Shape	Hexagon	Pentagonal pyramid	Octahedron	**Trigonal prism**	Johnson pentagonal pyramid J2
Symmetry	D_{6h}	C_{5v}	*Oh*	$\boldsymbol{D_{3h}}$	C_{5v}
Deviation	29.866	12.771	7.299	**7.135**	15.647

Table S9. Shape analysis in complex **6** (Na2 atom)

Structure	PP-5	vOC-5	**TBPY-5**	SPY-5	JTBPY-6
Shape	Pentagon	Vacant octahedron	**Trigonal bipyramid**	Spherical square pyramid	Johnson trigonal bipyramid J12

Symmetry	D_{5h}	C_{4v}	$\boldsymbol{D_{3h}}$	C_{4v}	D_{3h}
Deviation	33.251	5.948	**0.599**	3.921	2.909

Table S10. Shape analysis in complex **7** (Na1 atom)

Structure	HP-6	PPY-6	**OC-6**	TPR-6	JPPY-6
Shape	Hexagon	Pentagonal pyramid	**Octahedron**	Trigonal prism	Johnson pentagonal pyramid J2
Symmetry	D_{6h}	C_{5v}	$\boldsymbol{O_h}$	D_{3h}	C_{5v}
Deviation	27.817	27.700	**0.452**	15.963	30.740

Table S11. Shape analysis in complex **7** (Na2 atom)

Structure	HP-6	PPY-6	**OC-6**	TPR-6	JPPY-6
Shape	Hexagon	Pentagonal pyramid	**Octahedron**	Trigonal prism	Johnson pentagonal pyramid J2
Symmetry	D_{6h}	C_{5v}	$\boldsymbol{O_h}$	D_{3h}	C_{5v}
Deviation	28.196	27.843	**0.442**	16.030	30.896

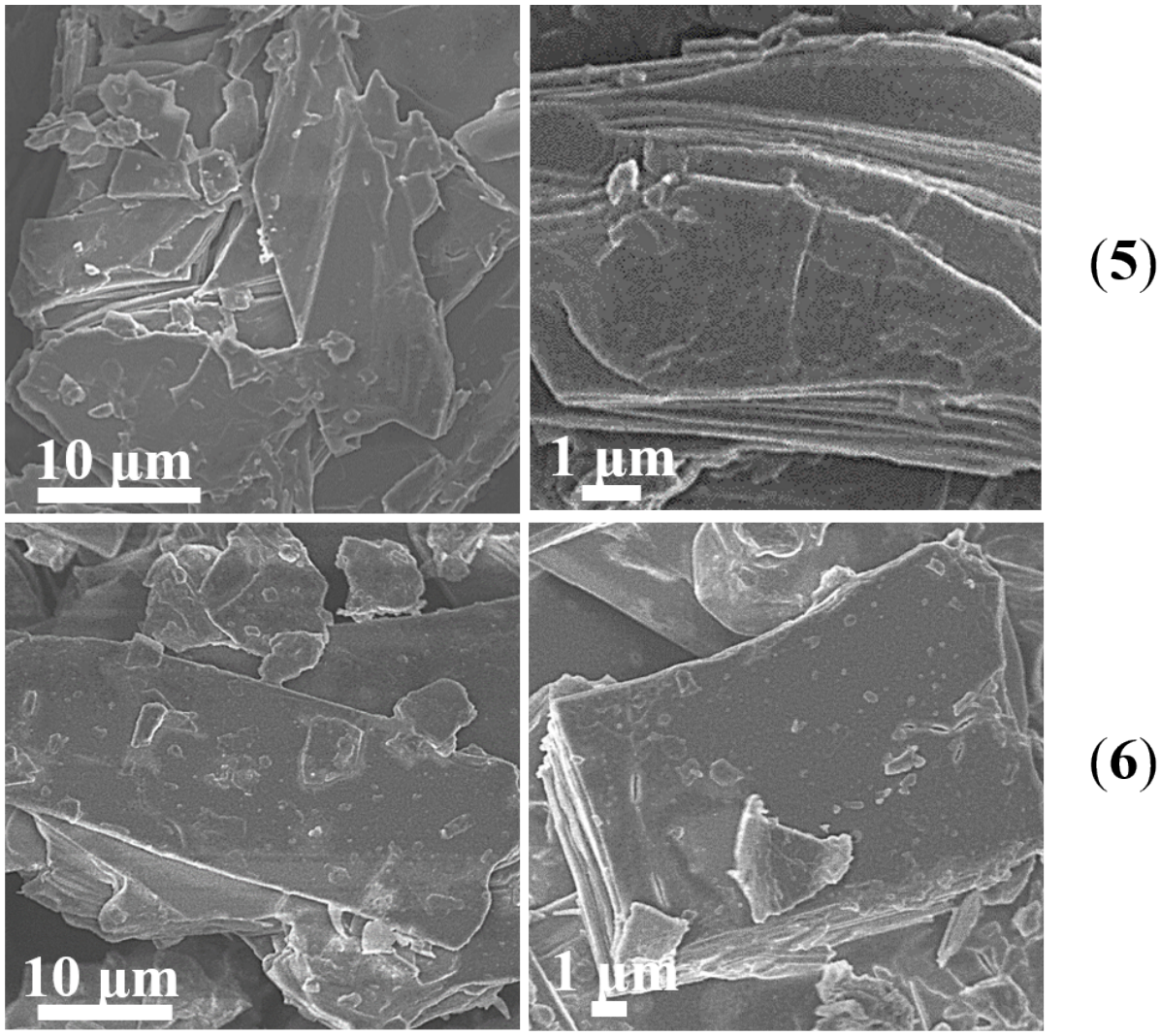

Figure S40. SEM images of **5** and **6** showing layered structures focus on the morphology of individual 2D sheets.

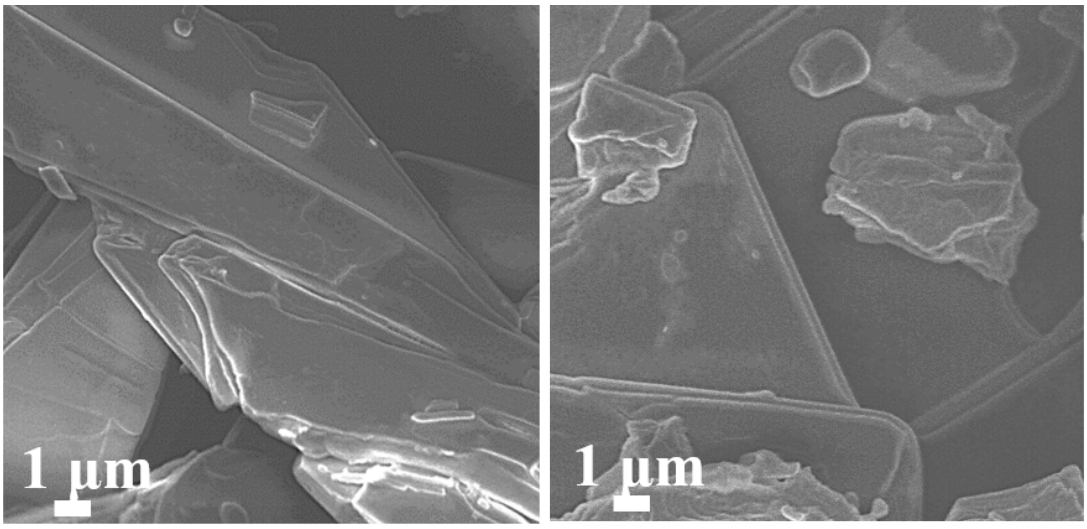

(7)

Figure S41. SEM images of **7** showing layered structures focus on the morphology of individual 2D sheets.

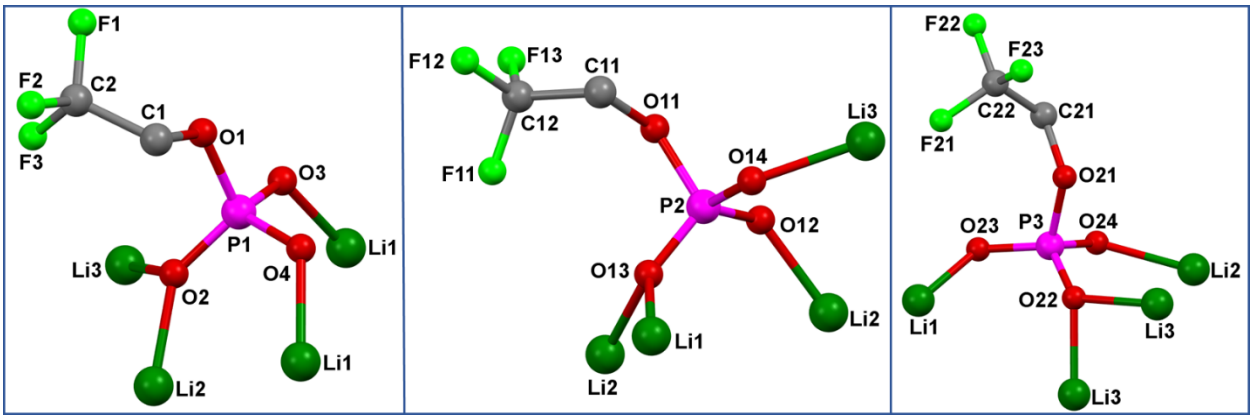

Figure S42. [4.1120] coordination mode of all the three phosphate ligands in **5**.

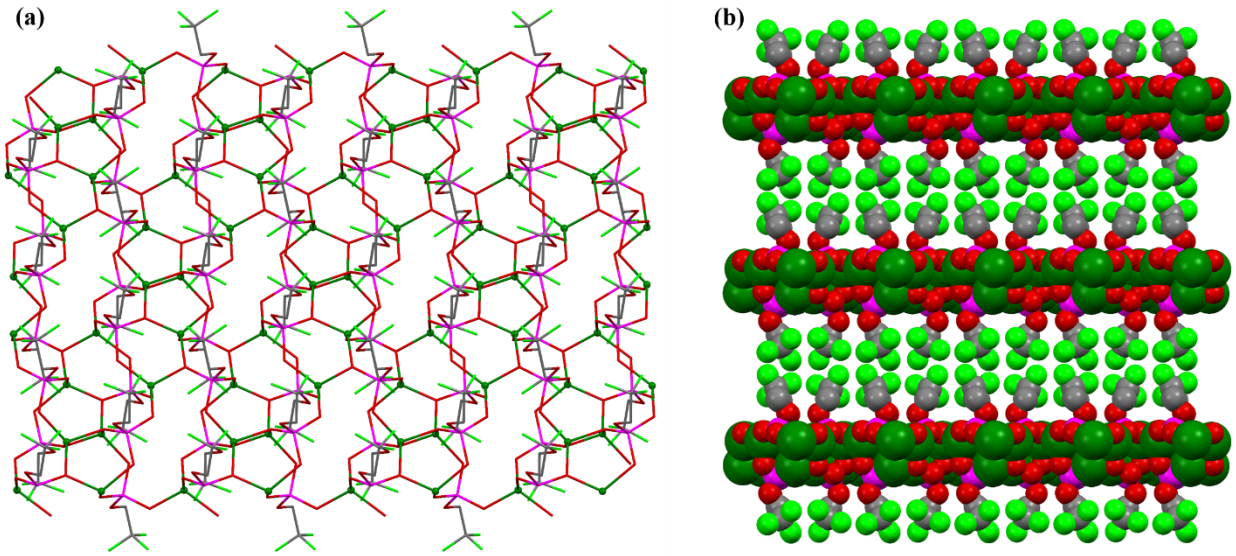

Figure S43. (a) Layered structure of Li fluoroethyl phosphate, view along the *c*-axis **5**; (C−H hydrogen atoms have been omitted for clarity); (b) Space-filling model showing the lattice arrangement of the layered structure of Li fluoroethyl phosphate, view along the *b*-axis.

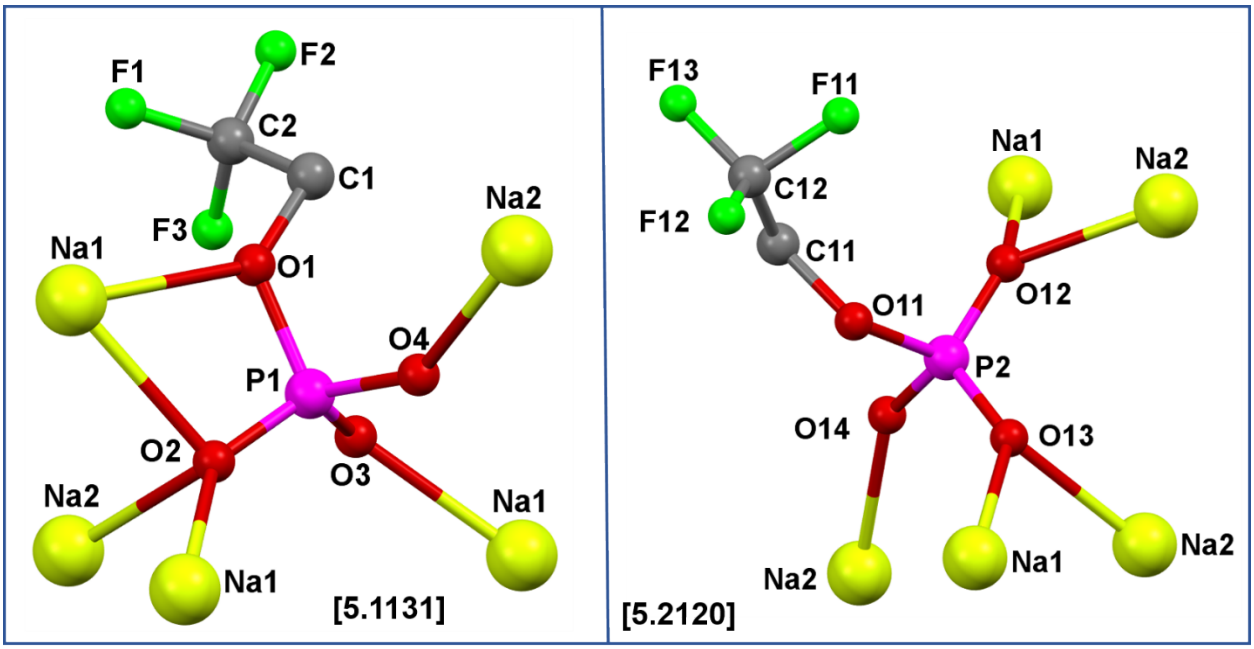

Figure S44. Possible coordination mode of trifluoroethyl phosphate ligands in **6**.

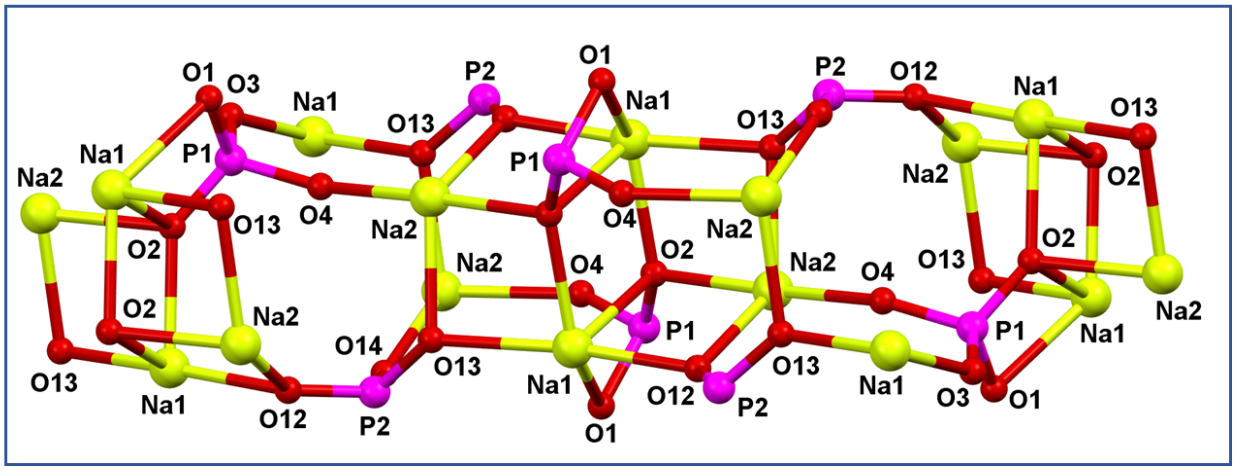

Figure S45. Core structure of the repeating unit of **6**; (C−H hydrogen atoms have been omitted for clarity) and some P2 coordinated oxygen atoms also omitted for clarity.

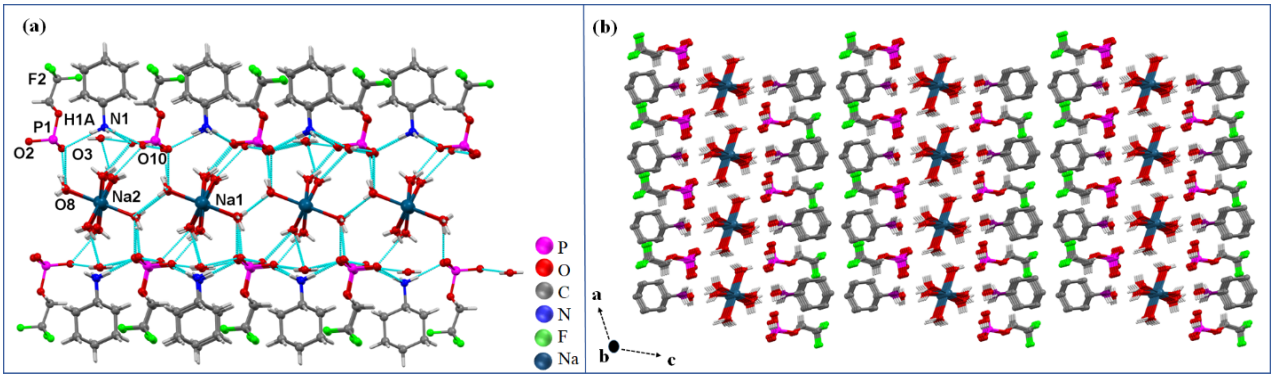

Figure S46. (a) H-Bonded supramolecular structure; (b) Layered structure of sodium fluoroethyl phosphate cyclohexylamine salt view along the *b*-axis.

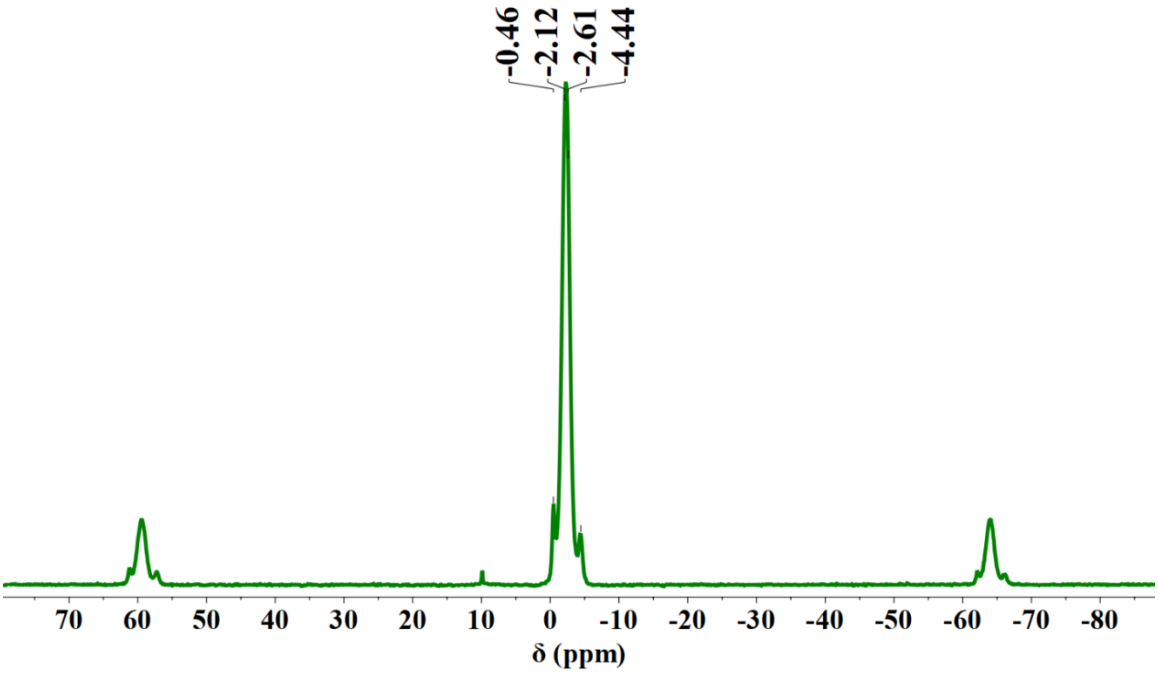

Figure S47. ^{31}P CP-MAS NMR spectrum of the decomposed product of **5 (**162 MHz).

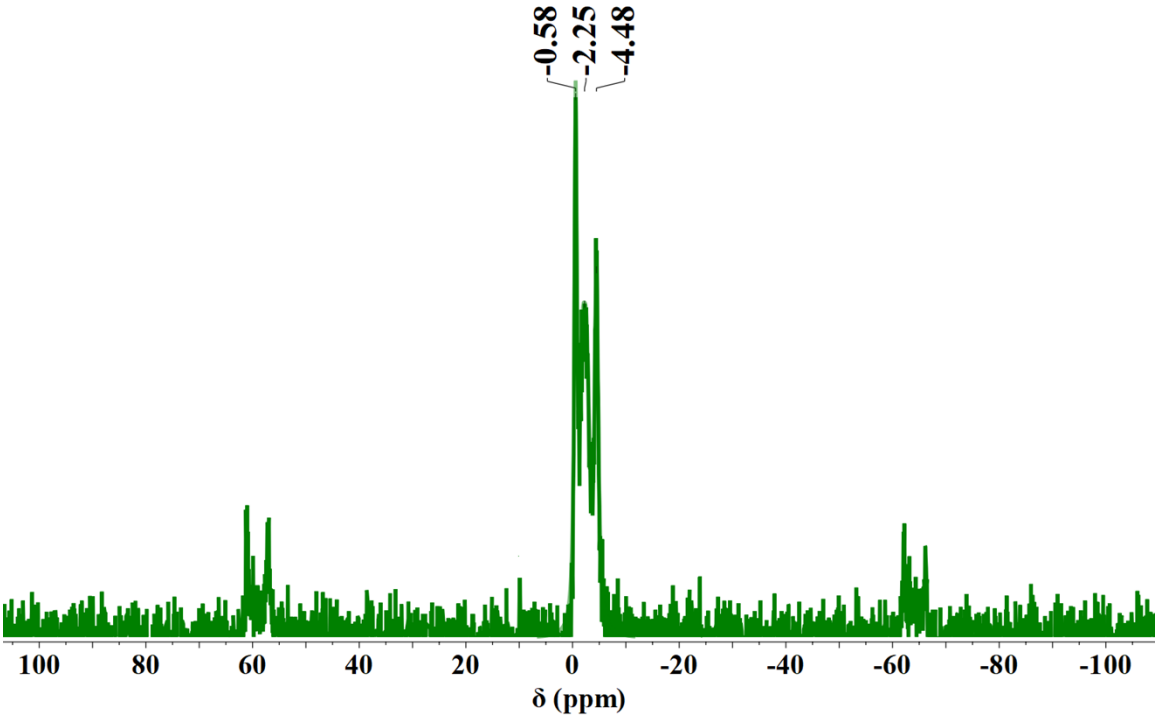

Figure S48. ^{31}P CP-MAS NMR spectrum of the decomposed product of **6 (**162 MHz).

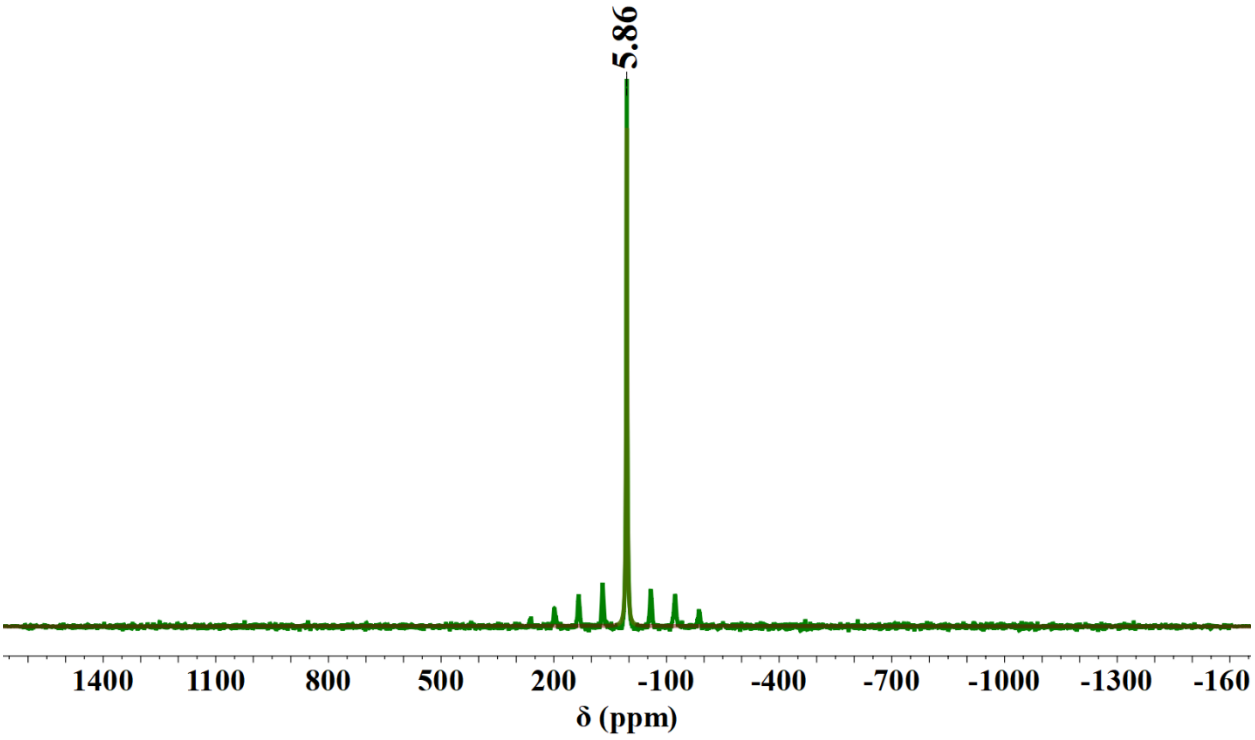

Figure S49. ^{7}Li CP-MAS NMR spectrum of the decomposed product of **5 (**155 MHz).

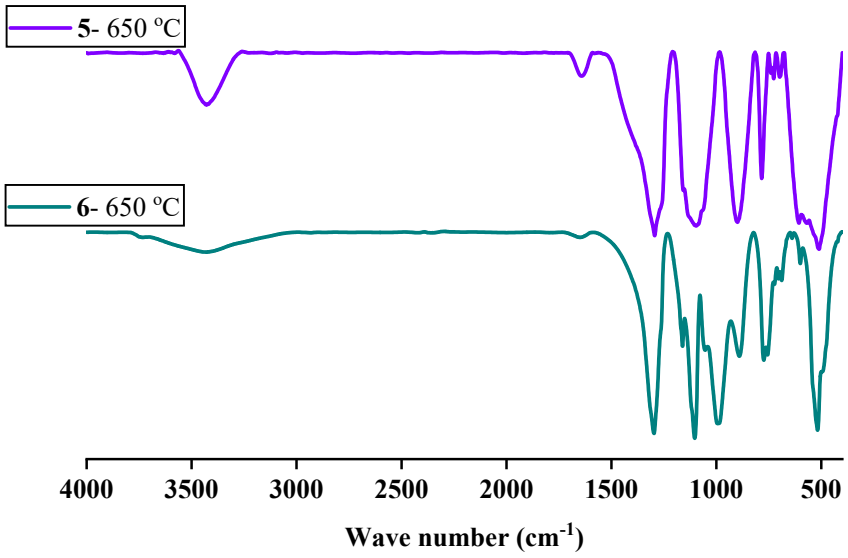

Figure S50. FT-IR spectra of the decomposed products of **5** and **6** (as KBr diluted discs).

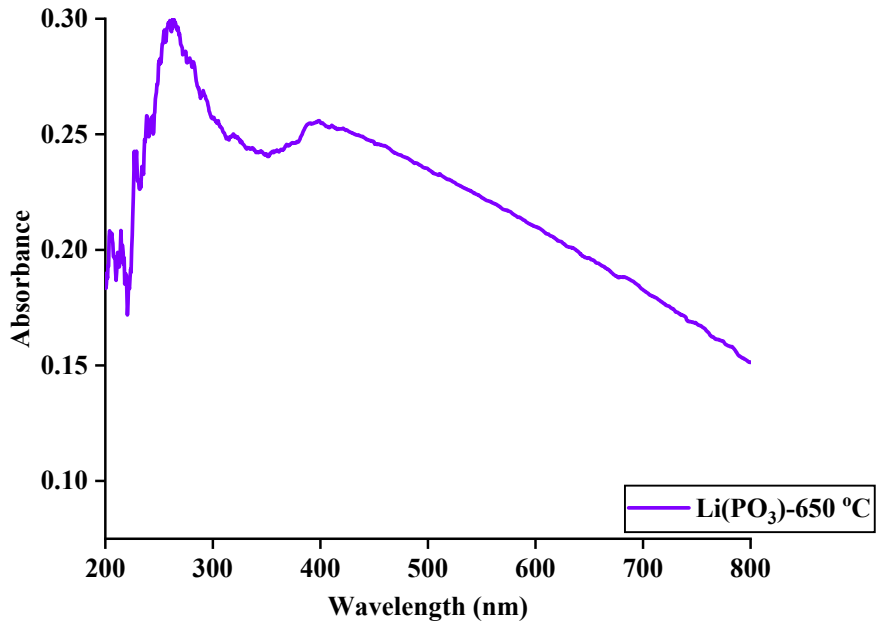

Figure S51. DR-UV spectrum of the decomposed product of **5** at 650 °C.

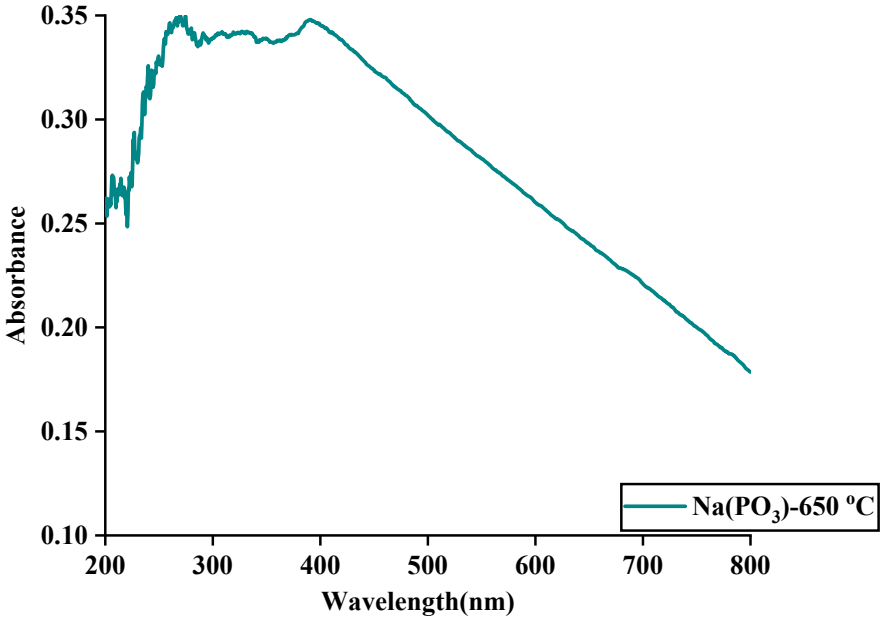

Figure S52. DR-UV spectrum of the decomposed product of **6** at 650 °C.

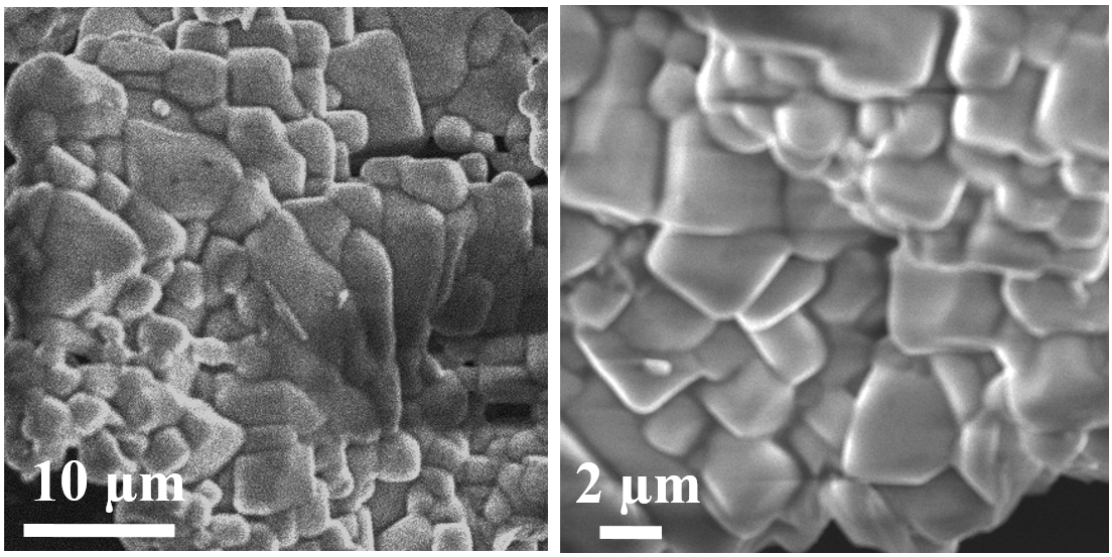

Figure 53. SEM of the decomposed product of **5** at 650 °C.

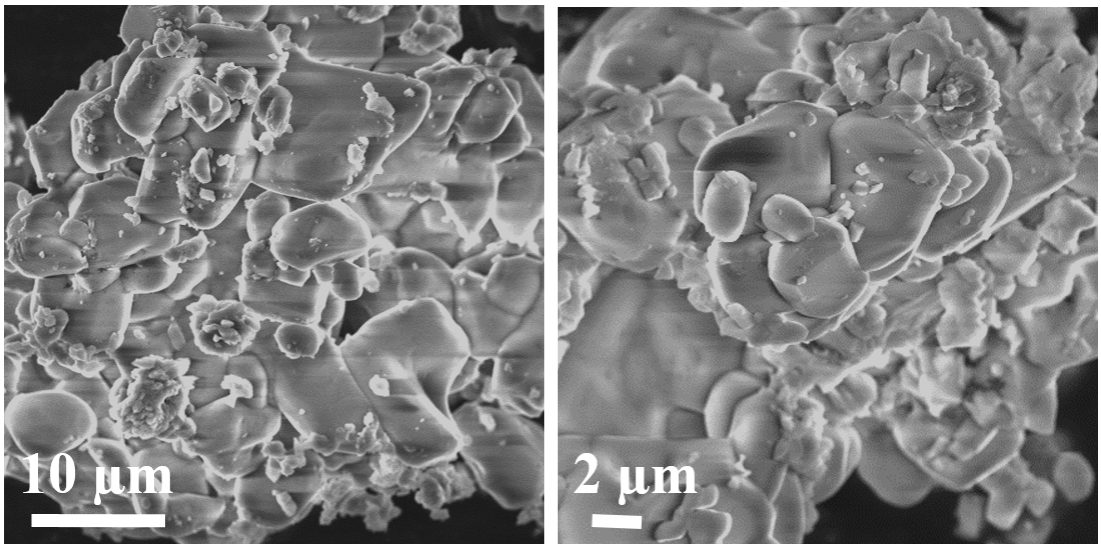

Figure 54. SEM of the decomposed product of **6** at 650 °C.

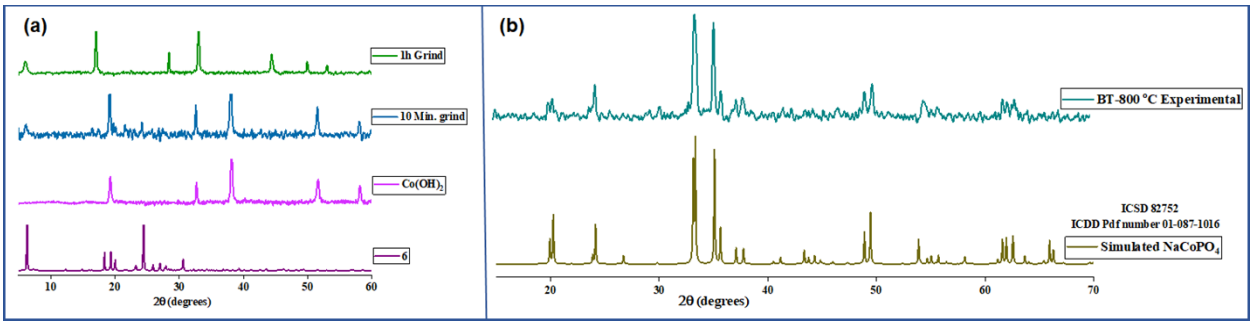

Figure S55. (a) PXRD pattern of the as-synthesized organophosphates $[(CF_3CH_2PO_4HNa)_2]_n$ **(6)** mixed with $Co(OH)_2$ and ground at different time intervals; (b) PXRD patterns of the heterometal decomposition products obtained after pyrolysis at 800 °C, along with associated reference patterns of BT- $NaCoPO_4$ (ICDD, PDF number 01-087-1016).

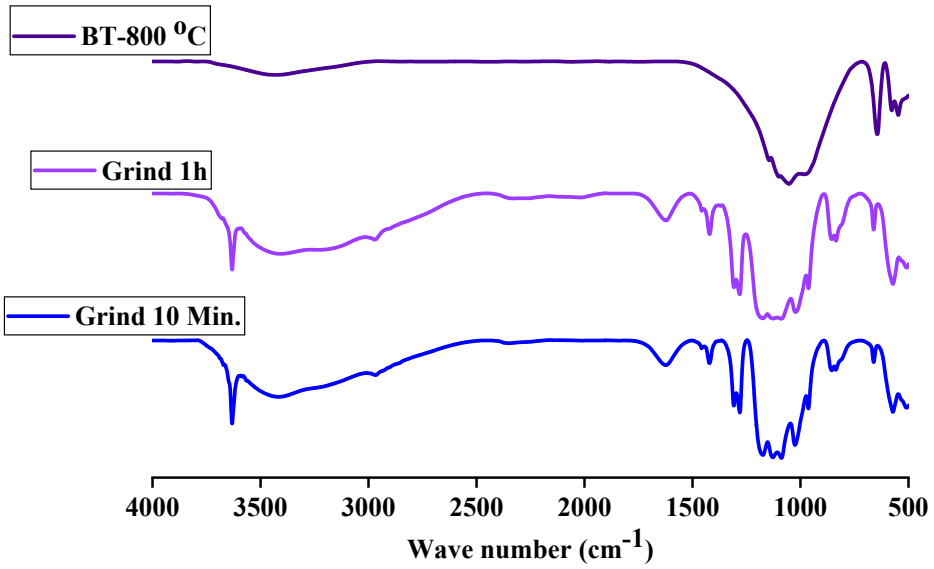

Figure S56. FT-IR spectra of compound **5** mixed with $Co(OH)_2$, ground for 10 Minutes, 1h, and BT-800 °C ($LiCoPO_4$) as KBr diluted discs.

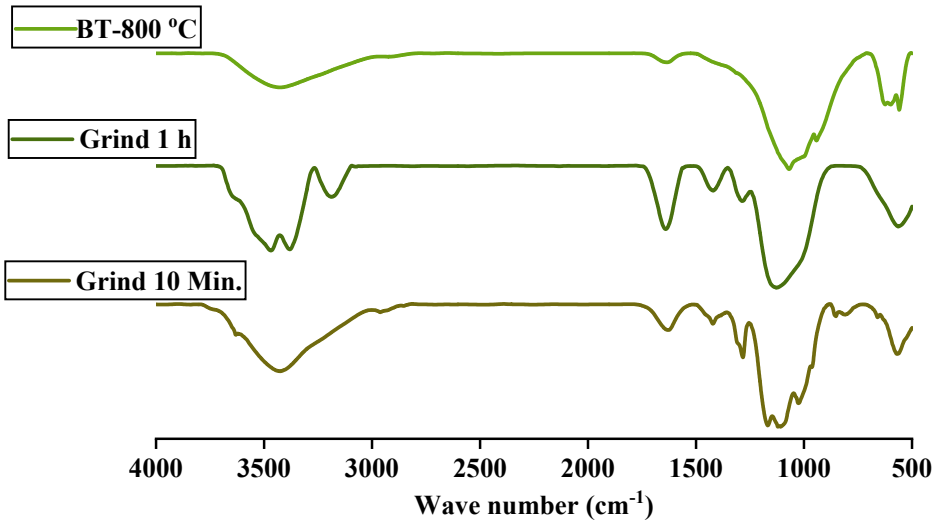

Figure S57. FT-IR spectra of compound **6** mixed with $Co(OH)_2$, ground for 10 Minutes, 1h, and BT-800 °C ($NaCoPO_4$) as KBr diluted discs.

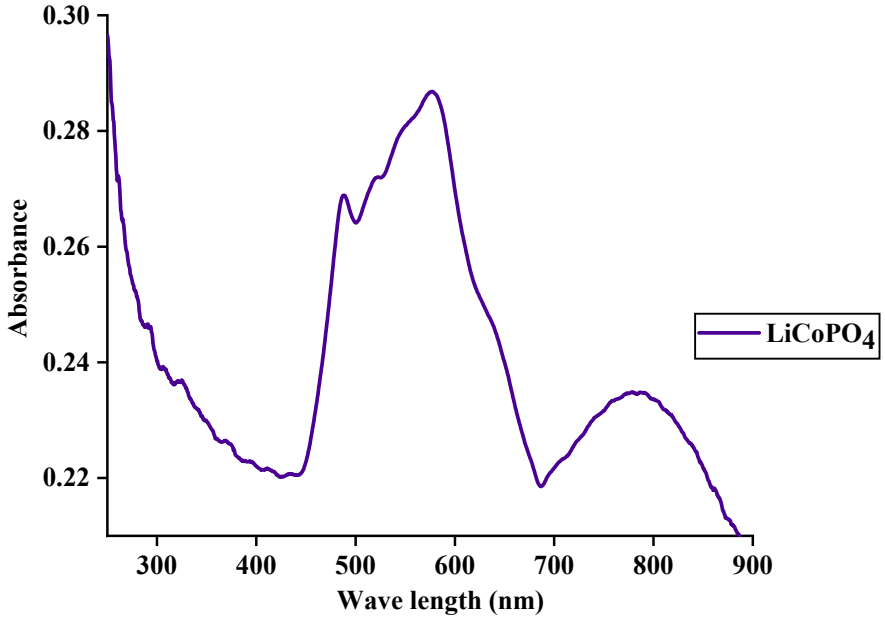

Figure S58. DR UV-Vis absorption spectrum of $LiCoPO_4$.

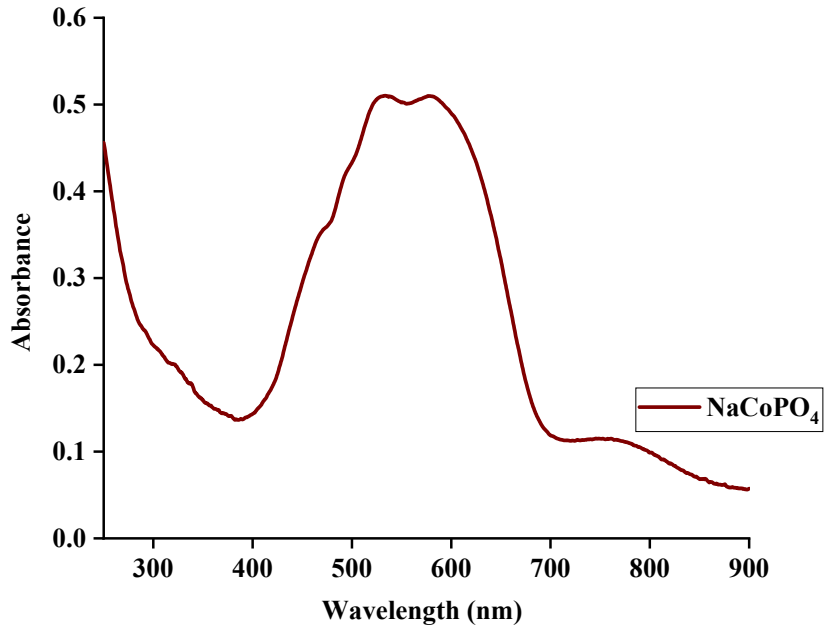

Figure S59. DR UV-Vis absorption spectrum of $NaCoPO_4$.

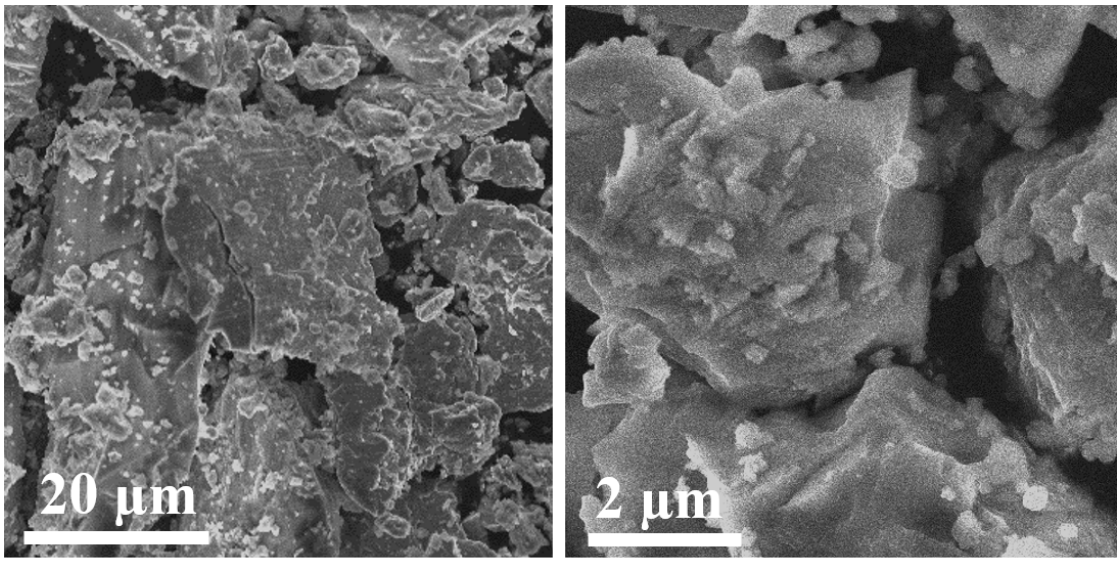

Figure S60. SEM of the product of BT-$LiCoPO_4$ at 800 °C.

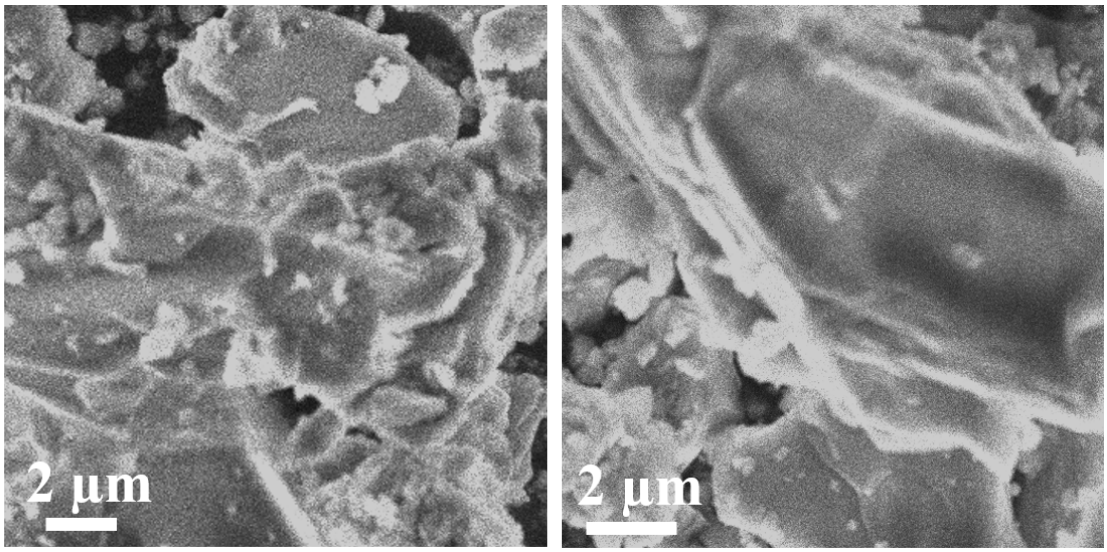

Figure S61. SEM of the product of BT-$NaCoPO_4$ at 800 °C.

Document: CP18062021 (varioMICRO) from: 18-06-2021 19:58:39

SP18022016
varioMICRO CHNS
serial number: 15154051

Graphic report

No.	Weight [mg]	Name	Method	C Area	H Area	C [%]	H [%]	C Factor	H Factor	Date Time	Info
39	1.5090	RM-AK-S30B	2mgChem80s	5 347	3 966	12.68	1.759	0.9723	1.0105	18-06-2021 18:25	Su

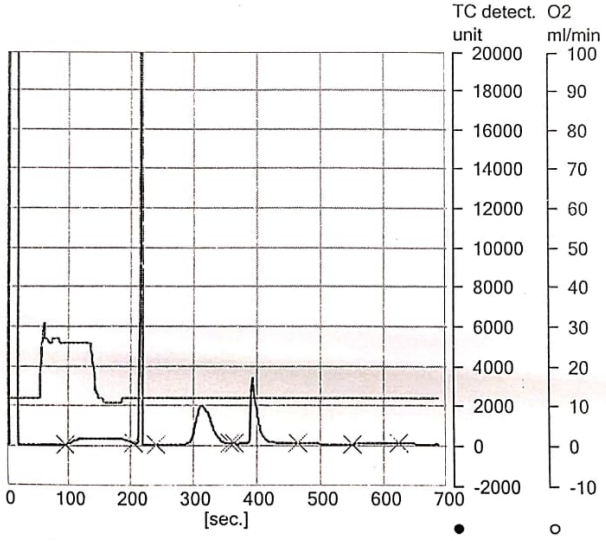

Figure S62. Elemental analysis of $[(CF_3CH_2PO_4HLi)_3]_n$ **(5)**.

No.	Weight [mg]	Name	Method	N Area	C Area	H Area	N [%]	C [%]	H [%]	Date Time	Info
20	1.2170	RM-AK-613-1	2mgChem80s	3 086	4 001	3 389	0.00	11.80	1.516	12-08-2021 14:13	

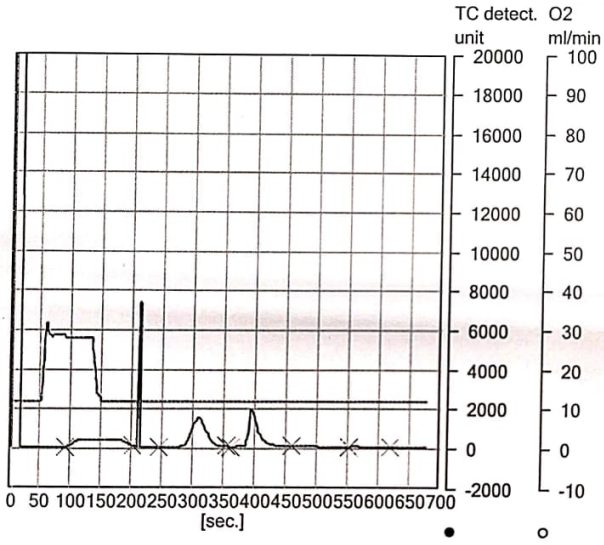

Name: eassuperuser, Access: VarioMICRO administrator

13-08-2021 14:20:54

varioMICRO V4.0.1 (aeb1e0e)2015-10-12, CHNS Mode, Ser. No.: 15154051
Elementar Analysensysteme GmbH

Page 3 (of 8)

Figure S63. Elemental analysis of $[(CF_3CH_2PO_4HNa)_2]_n$ (**6**).

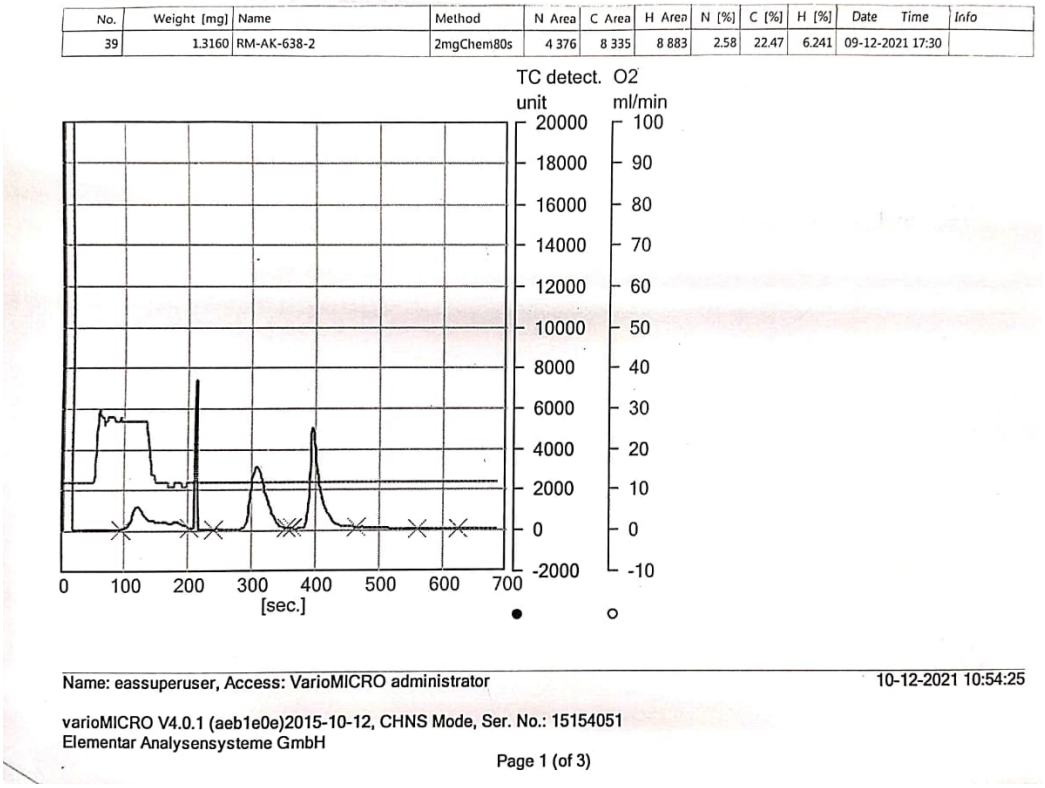

Figure S64. Elemental analysis of $[CF_3CH_2OPO_3(Na_{0.5})_2(CyNH_3)\cdot(H_2O)_6]_n$ (**7**).

Table S12: Selected bond distances (Å) and bond angles (°) in **1**.

P(1)–O(1)	1.634(3)	O2–P(1)–O(4)	113.5(1)
P(1)–O(2)	1.505(2)	O3–P(1)–O(1)	106.5(1)
P(1)–O(3)	1.515(2)	O3–P(1)–O(4)	112.4(1)
P(1)–O(4)	1.517(2)	O4–P(1)–O(1)	106.5(1)
F(1)–C(2)	1.337(5)	F(1)–C(2)–C(1)	111.8(4)
F(2)–C(2)	1.339(6)	F(2)–C(2)–C(1)	112.0(4)
F(3)–C(2)	1.332(5)	F(1)–C(2)–F(2)	106.3(4)
O(2)–P(1)–O(1)	102.6(1)	F(3)–C(2)–F(1)	106.8(4)

O(2)–P(1)–O(3)	114.3(1)	F(3)–C(2)–F(2)	106.4(4)

Table S13: Hydrogen bond table for **1** [Å and °].

D–H···A	d(D–H)	d(H···A)	d(D···A)	<(DHA)
O(5)–H(5C)···O(4)	0.86	1.93	2.781(3)	173.3
O(5) –H(5D)···O(4)$^{\#1}$	0.85	1.95	2.794(3)	171.3
N(1) –H(1A)···O(3)$^{\#2}$	0.91	1.83	2.722(3)	164.8
N(1) –H(1B)···O(2)$^{\#3}$	0.91	1.89	2.787(3)	167.7
N(1) –H(1C)···O(2)	0.91	1.83	2.744(3)	177.6
N(2) –H(2A)···O(3)$^{\#3}$	0.91	1.88	2.762(3)	162.2
N(2) –H(2B)···O(5)$^{\#4}$	0.91	1.92	2.755(3)	151.3
N(2) –H(2C)···O(4)$^{\#5}$	0.91	1.87	2.781(3)	175.1

Symmetry transformations used to generate equivalent atoms: $^{\#1}$3/2-X,1/2-Y,1-Z; $^{\#2}$+X,1+Y,+Z; $^{\#3}$3/2-X,1/2+Y,3/2-Z; $^{\#4}$+X,1-Y,1/2+Z; $^{\#5}$3/2-X,-1/2+Y,3/2-Z.

Table S14: Selected bond distances (Å) and bond angles (^{o}) in **2**.

P(1)–O(1)	1.575(3)	O(2) –P(1)–O(3)	114.8(3)
P(1)–O(2)	1.485(5)	O(2) –P(1)–O(4)	115.1(3)
P(1)–O(3)	1.534(5)	O(3) –P(1)–O(1)	105.4(3)
P(1)–O(4)	1.540(5)	O(3) –P(1)–O(4)	105.9(3)
F(1)–C(2)	1.331(9)	O(4) –P(1)–O(1)	109.3(3)
F(2)–C(2)	1.338(9)	F(1)–C(2)–F(2)	107.2(5)
F(3)–C(2)	1.350(8)	F(1)–C(2)–F(3)	107.0(6)
O(2) –P(1)–O(1)	105.8(3)	F(2)–C(2)–F(3)	107.1(5)

Table S15: Hydrogen bond table for **2** [Å and °].

D–H···A	d(D–H)	d(H···A)	d(D···A)	<(DHA)
O(3)–H(3)···O(2)$^{\#1}$	0.99(1)	1.69(1)	2.574(7)	147(1)

O(4) –H(4)···O(2)$^{\#2}$	0.84	1.89	2.571(7)	137.9

Symmetry transformations used to generate equivalent atoms: $^{\#1}$-1+X,+Y,+Z; $^{\#2}$-1-X,1/2+Y,-Z

Table S16: Selected bond distances (Å) and bond angles (°) in **3**.

P(1)–O(1)	1.603(3)	O(3)–P(1)–O(1)	100.5(2)
P(1)–O(2)	1.502(2)	O(3)–P(1)–O(2)	112.5(1)
P(1)–O(3)	1.512(2)	O(4)–P(1)–O(1)	108.0(2)
P(1)–O(4)	1.503(2)	O(4)–P(1)–O(2)	113.5(1)
O(2)–P(1)–O(1)	108.0(2)	O(4)–P(1)–O(3)	113.3(1)

Table S17: Hydrogen bond table for **3** [Å and °].

D−H···A	d(D−H)	d(H···A)	d(D···A)	<(DHA)
O(5)–H(5d)···O(4)	0.8708	1.826(11)	2.685(4)	168(5)
O(5) –H(5e)···O(6)$^{\#1}$	0.8698	1.914(5)	2.782(4)	175(4)
O(6) –H(6a)···O(5)	0.8400	1.781(7)	2.614(4)	171(4)
N(1) –H(1d)···O(3)	0.9100	1.773(4)	2.682(4)	176.8(8)
N(1) –H(1e)···O(4)$^{\#2}$	0.9100	1.790(5)	2.689(4)	168.8(19)
N(2) –H(2a)···O(2)$^{\#2}$	0.9100	1.840(4)	2.747(3)	174.3(18)
N(2) –H(2b)···O(2)$^{\#3}$	0.9100	1.846(6)	2.743(4)	168.2(19)
N(2) –H(2c)···O(3)	0.9100	1.835(4)	2.739(3)	171.5(7)

Symmetry transformations used to generate equivalent atoms: $^{\#1}$3/2-X,1/2+Y,3/2-Z; $^{\#2}$+X,1+Y,+Z; $^{\#3}$1/2-X,1/2+Y,3/2-Z.

Table S18: Selected bond distances (Å) and bond angles (°) in **4**.

P(1)–O(1)	1.564(2)	O(2)–P(1)–O(3)	114.63(9)
P(1)–O(2)	1.499(2)	O(2)–P(1)–O(4)	112.52(9)
P(1)–O(3)	1.543(2)	O(3)–P(1)–O(1)	104.01(8)
P(1)–O(4)	1.542(2)	O(4)–P(1)–O(1)	106.95(9)
O(2)–P(1)–O(1)	112.03(9)	O(4)–P(1)–O(3)	106.01(9)

Table S19: Hydrogen bond table for **4** [Å and °].

D−H···A	d(D−H)	d(H···A)	d(D···A)	<(DHA)
O(3)–H(3)···O(2)$^{\#1}$	0.84	1.77	2.604(2)	175.7
O(4) –H(4)···O(2)$^{\#2}$	0.84	1.76	2.587(2)	165.9

Symmetry transformations used to generate equivalent atoms: $^{\#1}$1-X,-1/2+Y,3/2-Z; $^{\#2}$1-X,1-Y,1-Z.

Table S20: Selected bond distances (Å) and bond angles (°) in **5**.

P(1)– O(1)	1.587(3)	F(21) –C(22)	1.335(6)
P(1)–O(2)	1.489(4)	F(22) –C(22)	1.334(6)
P(1)–O(3)	1.507(3)	F(23) –C(22)	1.327(6)
P(1)–O(4)	1.577(3)	F(1) –C(2) –F(2)	107.1(5)
P(2)–O(11)	1.587(3)	F(1) –C(2) –F(3)	107.2(5)
P(2)–O(12)	1.491(3)	F(3) –C(2) –F(2)	106.2(4)
P(2)–O(13)	1.493(3)	F(11) –C(12) –F(12)	106.5(4)
P(2)–O(14)	1.589(3)	F(11) –C(12) –F(13)	105.9(4)
P(3) –O(21)	1.590(3)	F(13) –C(12) –F(12)	106.6(4)
P(3) –O(22)	1.485(3)	F(22) –C(22) –F(21)	106.9(4)
P(3) –O(23)	1.501(3)	F(23) –C(22) –F(21)	106.6(4)
P(3) –O(24)	1.576(3)	F(23) –C(22) –F(22)	107.2(5)
Li(2)$^{\#4}$–O(2)	1.920(8)	O(3)–Li(1)–O(4)$^{\#5}$	105.1(4)
Li(3)$^{\#1}$–O(2)	2.005(9)	O(13)–Li(1)–O(2)$^{\#5}$	113.1(4)
Li(1)$^{\#5}$–O(4)	2.036(9)	O(13)–Li(1)–O(3)	107.3(4)
Li(1)–O(3)	1.947(9)	O(23)–Li(1)–O(4) $^{\#5}$	118.3(4)
Li(2)–O(12)	1.945(9)	O(23)–Li(1)–O(3)	110.8(4)
Li(1)–O(13)	1.924(8)	O(23)–Li(1)–O(13)	102.0(4)
Li(2)$^{\#2}$–O(13)	1.955(8)	O(2)$^{\#6}$–Li(2)–O(12)	102.0(4)
Li(3)$^{\#6}$–O(14)	2.009(8)	O(2)$^{\#6}$–Li(2)–O(13)$^{\#2}$	108.9(4)
Li(3)$^{\#1}$–O(22)	1.935(9)	O(2)$^{\#6}$–Li(2)–O(24)$^{\#3}$	114.1(4)

Li(3)–O(22)	1.917(8)	O(12)–Li(2)–O(13)$^{\#2}$	115.7(4)
Li(1) –O(23)	1.922(8)	O(12)–Li(2)–O(24)$^{\#3}$	105.1(4)
Li(2)$^{\#3}$–O(24)	2.036(8)	O(13)$^{\#2}$–Li(2)–O(24)$^{\#3}$	110.9(4)
F(1) –C(2)	1.316(6)	O(2)$^{\#1}$–Li(3)–O(14)$^{\#4}$	116.2(4)
F(2) –C(2)	1.335(6)	O(22)–Li(3)–O(2)$^{\#1}$	107.5(4)
F(3) –C(2)	1.333(6)	O(22)$^{\#1}$–Li(3)–O(2)$^{\#1}$	119.0(4)
F(11) –C(12)	1.328(6)	O(22)–Li(3)–O(14)$^{\#4}$	114.2(4)
F(12) –C(12)	1.339(6)	O(22)$^{\#1}$–Li(3)–O(14)$^{\#4}$	104.5(4)
F(13) –C(12)	1.335(6)	O(22)–Li(3)–O(22)$^{\#1}$	93.5(4)

Symmetry transformations used to generate equivalent atoms: $^{\#1}$1-X,2-Y,1-Z; $^{\#2}$2-X,1-Y,1-Z; $^{\#3}$2-X,2-Y,1-Z; $^{\#4}$-1+X,+Y,+Z; $^{\#5}$1-X,1-Y,1-Z; $^{\#6}$1+X,+Y,+Z.

Table S21: Hydrogen bond table for **5** [Å and °].

D−H···A	d(D−H)	d(H···A)	d(D···A)	<(DHA)
O(4)–H(4)···O(12)$^{\#1}$	0.84	1.77	2.609(4)	174.5
O(14) –H(14)···O(23)	0.838	1.77	2.592(4)	165
O(24) –H(24)···O(3)$^{\#2}$	0.84	1.72	2.559(4)	172.8

Symmetry transformations used to generate equivalent atoms: $^{\#1}$2-X,1-Y,1-Z; $^{\#2}$2-X,2-Y,1-Z.

Table S22: Selected bond distances (Å) and bond angles (^{o}) in **6**.

P(1)–O(1)	1.604(4)	O(13)–P(2)–O(11)	104.3(2)
P(1) –O(2)	1.487(4)	O(13)–P(2)–O(14)	109.3(3)
P(1) –O(3)	1.501(4)	O(14)–P(2)–O(11)	104.2(2)
P(1) –O(4)	1.582(4)	O(2)$^{\#1}$– Na(1)– O(1)$^{\#1}$	57.2(1)
P(2)–O(11)	1.606(5)	O(2)– Na(1)– O(1)$^{\#1}$	129.3(2)
P(2)–O(12)	1.486(5)	O(2)– Na(1)– O(2)$^{\#1}$	79.2(2)
P(2)–O(13)	1.509(4)	O(2)– Na(1)– O(3)$^{\#3}$	95.3(2)
P(2)–O(14)	1.562(4)	O(2)– Na(1)– O(12)	99.7(2)

F(1) –C(2)	1.340(1)	O(2)– Na(1)– O(13)$^{\#4}$	82.4(2)
F(2) –C(2)	1.329(9)	O(3)$^{\#3}$– Na(1)– O(1)$^{\#1}$	132.4(2)
F(3) –C(2)	1.337(1)	O(3) $^{\#3}$– Na(1)– O(2)$^{\#1}$	167.2(2)
F(11) –C(12)	1.422(1)	O(3) $^{\#3}$– Na(1)– O(13) $^{\#4}$	84.5(2)
F(12) –C(12)	1.249(1)	O(12)– Na(1)– O(1)$^{\#1}$	100.7(2)
F(13) –C(12)	1.333(9)	O(12)– Na(1)– O(2)$^{\#1}$	84.7(2)
Na(1) –O(1)$^{\#1}$	2.533(5)	O(12) – Na(1)– O(3)$^{\#3}$	84.9(2)
Na(1) –O(2)$^{\#1}$	2.519(5)	O(12) – Na(1)– O(13)$^{\#4}$	169.3(2)
Na(1) –O(2)	2.334(5)	O(13)$^{\#4}$ – Na(1)– O(1)$^{\#1}$	85.8(2)
Na(1) –O(3) $^{\#3}$	2.374(5)	O(13) $^{\#4}$– Na(1)– O(2)$^{\#1}$	106.0(2)
Na(1) –O(12)	2.351(4)	O(14) $^{\#6}$– Na(2)– O(2)$^{\#1}$	89.3(2)
Na(1) –O(13) $^{\#4}$	2.463(4)	O(14) $^{\#6}$– Na(2)– O(4)$^{\#5}$	98.1(2)
Na(2)–O(2) $^{\#1}$	2.413(4)	O(2)$^{\#1}$ – Na(2)– O(4)$^{\#5}$	172.6(2)
Na(2)–O(4) $^{\#5}$	2.438(5)	O(12)– Na(2)– O(2)$^{\#1}$	88.3(2)
Na(2)–O(12)	2.297(5)	O(12)– Na(2)– O(4)$^{\#5}$	87.3(2)
Na(2)–O(13)$^{\#5}$	2.351(5)	O(12)– Na(2)– O(13)$^{\#5}$	123.9(2)
Na(2)–O(14) $^{\#6}$	2.377(5)	O(12)– Na(2)– O(14)$^{\#6}$	125.3(2)
O(12)–P(2)–O(14)	111.5(2)	O(13)$^{\#5}$– Na(2)– O(2)$^{\#1}$	83.08(2)
O(2)–P(1)–O(1)	103.0(2)	O(13) $^{\#5}$– Na(2)– O(4)$^{\#5}$	94.5(2)
O(2)–P(1)–O(3)	117.9(2)	O(13) $^{\#5}$– Na(2)– O(14)$^{\#6}$	110.0(2)
O(2)–P(1)–O(4)	112.7(3)	F(2)– C(2)–F(1)	108.3(7)
O(3)–P(1)–O(1)	110.4(2)	F(2)– C(2)–F(3)	108.5(8)
O(3)–P(1)–O(4)	107.7(2)	F(3)– C(2)–F(1)	107.2(7)
O(4)–P(1)–O(1)	104.3(2)	F(12) – C(12)–F(11)	101.4(9)
O(12)–P(2)–O(11)	110.0(3)	F(12) – C(12)–F(13)	109.7(8)
O(12)–P(2)–O(13)	116.5(2)	F(13) – C(12)–F(11)	103.5(8)
O(12)–P(2)–O(14)	111.5(2)		

Symmetry transformations used to generate equivalent atoms: #1 1-X,1-Y,1-Z; #2 1-X,1/2+Y,1/2-Z; #3 1-X,2-Y,1-Z; #4 +X,3/2-Y,1/2+Z; #5 1-X,-1/2+Y,1/2-Z; #6 +X,-1+Y,+Z; #7 +X,1+Y,+Z; #8 +X,3/2-Y,-1/2+Z.

Table S23: Hydrogen bond table for **6** [Å and °].

D−H···A	d(D−H)	d(H···A)	d(D···A)	<(DHA)
O(14)–H(14)···O(3)#1	0.76(8)	1.76(8)	2.510(6)	169(9)
O(4)–H(4)···O(13)#2	0.99(8)	1.60(8)	2.580(6)	172(7)

Symmetry transformations used to generate equivalent atoms: #1 1-X,1/2+Y,1/2-Z; #2 1-X,2-Y,1-Z

Table S24: Selected bond distances (Å) and bond angles (°) in **7**.

P(1)–O(1)	1.636(2)	O(8) –Na(1) –O(8) #2	180.0
P(1) –O(2)	1.515(2)	O(8) –Na(1) –O(5) #2	87.5(8)
P(1) –O(3)	1.515(2)	O(8)#2–Na(1) –O(5)	87.5(8)
P(1) –O(4)	1.515(2)	O(8)#2–Na(1) –O(5)#2	92.5(8)
F(1)–C(2)	1.342(3)	O(8)–Na(1) –O(5)	92.5(8)
F(2)–C(2)	1.329(3)	O(8)–Na(1) –O(7)	85.0(8)
F(3)–C(2)	1.345(3)	O(8)#2–Na(1) –O(7)	95.0(8)
Na(1)– O(8) #2	2.366(2)	O(8) #2–Na(1) –O(7)#2	95.0(8)
Na(1) – O(8)	2.366(2)	O(5)–Na(1) –O(5)#2	180.0(8)
Na(1) – O(5)	2.421(2)	O(5) #2–Na(1)–O(7)#2	82.4(7)
Na(1) – O(5)#2	2.421(2)	O(5)#2–Na(1) –O(7)	92.6(7)
Na(1) – O(7) #2	2.458(2)	O(5)–Na(1) –O(7)#2	97.6(7)
Na(1) – O(7)	2.458(2)	O(5)–Na(1) –O(7)	82.4(7)
Na(2) – O(5) #3	2.441(2)	O(7) #2–Na(1) –O(7)	180.0
Na(2) – O(5)	2.441(2)	O(5)#4–Na(2) –O(5)	180.0
Na(2) – O(6) #3	2.370(2)	O(5)–Na(2) –O(7)	81.9(7)

Na(2) – O(6)	2.371(2)	O(5)$^{\#4}$–Na(2) –O(7)$^{\#4}$	81.9(7)
Na(2) – O(7)	2.464(2)	O(5)–Na(2) –O(7)$^{\#4}$	98.2(7)
Na(2) – O(7) $^{\#3}$	2.464(2)	O(5)$^{\#4}$–Na(2) –O(7)	98.2(7)
N(1) – C(3)	1.496(4)	O(6)–Na(2) –O(5)$^{\#4}$	92.2(8)
F(1)–C(2) –F(3)	107.4(2)	O(6)$^{\#4}$–Na(2) –O(5)	92.2(8)
F(2) –C(2) –F(1)	106.9(2)	O(6)–Na(2) –O(5)	87.9(8)
F(2) –C(2) –F(3)	106.9(2)	O(6)$^{\#4}$–Na(2) –O(5) $^{\#4}$	87.9(8)
O(2) –P(1) –O(1)	106.3(1)	O(6) $^{\#4}$–Na(2) –O(6)	180.0
O(2) –P(1) –O(3)	113.5(1)	O(6) $^{\#4}$–Na(2) –O(7) $^{\#4}$	93.5(8)
O(2) –P(1) –O(4)	114.8(1)	O(6)–Na(2) –O(7)$^{\#4}$	86.6(8)
O(3) –P(1) –O(1)	105.6(1)	O(6) $^{\#4}$–Na(2) –O(7)	180.0(1)
O(4) –P(1) –O(1)	102.5(1)	O(6)–Na(2) –O(7)	86.6(8)
O(4) –P(1) –O(3)	112.8(1)		

Symmetry transformations used to generate equivalent atoms:. ^{1}+X,1+Y,+Z; ^{2}1-X,1-Y,1-Z; ^{3}+X,-1+Y,+Z; ^{4}1-X,-Y,1-Z

Table S25: Hydrogen bond table for **7** [Å and °].

D–H···A	d(D–H)	d(H···A)	d(D···A)	<(DHA)
O(7) –H(7C)···O(9)	0.82(6)	2.03(6)	2.832(3)	166(6)
O(8) –H(8C)···O(8)$^{\#1}$	0.95	2.41	2.713(4)	98.1
O(8) –H(8D)···O(4)	0.95	1.98	2.795(3)	143.2
O(5) –H(5D)···O(2)$^{\#1}$	0.87(5)	1.92(5)	2.765(3)	161(4)
O(6) –H(6C)···O(3)$^{\#2}$	0.85	1.86	2.712(3)	173.5
O(6) –H(6D)···O(8) $^{\#3}$	0.85	1.94	2.775(3)	165.2
O(7) –H(7D)···O(10)	0.76(5)	2.19(5)	2.849(3)	144(4)
O(9) –H(9A)···O(3)$^{\#4}$	0.85	1.94	2.760(3)	162.6
O(10) –H(10A)···O(3)$^{\#5}$	0.85	1.92	2.763(3)	171.7
O(10) –H(10B)···O(4)$^{\#6}$	0.85	2.00	2.825(3)	162.7
N(1) –H(1A)···O(4)	0.91	1.92	2.826(3)	175.4
N(1) –H(1C)···O(2)$^{\#6}$	0.91	1.96	2.857(3)	167.6

Symmetry transformations used to generate equivalent atoms:. [1]-X,1-Y,1-Z; [2]1-X,-Y,1-Z; [3]2-X,-Y,1-Z; [4]1-X,1-Y,1-Z; [5]+X,-1+Y,+Z; [6]1+X,-1+Y,+Z; [7]1+X,+Y,+Z.

References

1. M. J. Turner, J. J. McKinnon, S. K. Wolff, D. J. Grimwood, P. R. Spackman, D. Jayatilaka and M. A. Spackman, *Journal*, 2017.
2. A. J. Edwards, C. F. Mackenzie, P. R. Spackman, D. Jayatilaka and M. A. Spackman, *Faraday Discuss.*, 2017, **203**, 93-112.
3. M. A. Spackman and D. Jayatilaka, *CrystEngComm*, 2009, **11**, 19-32.
4. J. J. Koenderink, *Cambridge, MA, USA.*, 1990.